

Bayesian Hierarchical Modeling for Bivariate Multiscale Spatial Data with Application to Blood Test Monitoring

Shijie Zhou* and Jonathan R. Bradley†

Abstract

In public health applications, spatial data collected are often recorded at different spatial scales and over different correlated variables. Spatial change of support is a key inferential problem in these applications and have become standard in univariate settings; however, it is less standard in multivariate settings. There are several existing multivariate spatial models that can be easily combined with multiscale spatial approach to analyze multivariate multiscale spatial data. In this paper, we propose three new models from such combinations for bivariate multiscale spatial data in a Bayesian context. In particular, we extend spatial random effects models, multivariate conditional autoregressive models, and ordered hierarchical models through a multiscale spatial approach. We run simulation studies for the three models and compare them in terms of prediction performance and computational efficiency. We motivate our models through an analysis of 2015 Texas annual average percentage receiving two blood tests from the Dartmouth Atlas Project.

Keywords: *Change of support; Image segmentation; Regionalization; Simple areal interpolation; Spatial misalignment.*

1 Introduction

Multiscale spatial analysis has gained attention in spatial, spatio-temporal statistics, and many subject matter domains over the past decades (see Waller & Gotway, 2004 for a standard reference). The term “multiscale” refers to the case when more than one spatial resolution is involved in the analysis. By multivariate multiscale spatial data, we mean we observe more than one spatial response at multiple spatial scales. For example, the Dartmouth Atlas dataset provides data on hospital service areas (HSA), counties, and other

* (Corresponding author) Email: sz20bh@fsu.edu. Department of Statistics, Florida State University, 117 N. Woodward Ave., Tallahassee, Florida, U.S.A.

† Email: jrbradley@fsu.edu. Department of Statistics, Florida State University, 117 N. Woodward Ave., Tallahassee, Florida, U.S.A.

pre-defined regions for several variables, including the average annual percentage of diabetic Medicare enrollees aged 65-75 having hemoglobin A1c test and the average annual percentage of diabetic Medicare enrollees aged 65-75 having blood lipids (LDL-C) test (Dartmouth Atlas Data, 2022).

We are motivated by this data on the annual average percentage of individuals receiving certain blood tests since blood tests play a crucial role during the treatment of diabetes. Certain blood tests, such as the hemoglobin A1c test, are considered to be the standard measures of diabetes management (Delamater, 2006) and regular measurements are shown to be beneficial to diabetes control (Larsen et al., 1990). Considering the importance of blood tests for diabetic patients, our goal is to jointly analyze the average annual percentage of individuals receiving the two blood tests on different spatial scales from the Dartmouth Atlas Project. To achieve this goal, one needs to combine existing methodologies in a novel way. In particular, we consider combining several multivariate spatial models with a multiscale spatial approach to analyze such bivariate multiscale spatial data.

In univariate settings, a typical multiscale problem occurs when we observe data at one scale but are instead interested in conducting inference on another scale. This is commonly known as the spatial change of support (COS) problem (see Gotway & Young, 2002 for a comprehensive review). One type of COS is to use data collected at one areal scale to predict on another areal scale. These two scales are often misaligned in practice, and COS is achieved through a partitioning of the available supports (i.e., source supports) and the support for inference (i.e., target support), and assuming the process is piece-wise constant over this partitioning (Mugglin & Carlin, 1998; Mugglin et al., 1999). There are other types of COS and multiscale approaches such as points-to-regions prediction where COS can be achieved by integrating the point process up to an areal support (Benedetti et al., 2022; Bradley et al., 2017; Gelfand et al., 2001; Qu et al., 2021; Wikle & Berliner, 2005); however, this type of multiscale features are not present in the Dartmouth Atlas Data. Our goal is to develop innovative bivariate multiscale spatial models through combining standard multivariate spatial models with the appropriate multiscale approach for correlated spatial responses observed over spatially misaligned areal scales.

We mainly consider three multivariate spatial models: the spatial random effects model (Cressie & Johannesson, 2008), the multivariate conditional autoregressive (MCAR) model (Gelfand & Vounatsou, 2003), and ordered (by variable) hierarchical model (Royle & Berliner, 1999). In the spatial random effects model, dependence between variables is induced through a mean-zero random vector shared across all locations and variables. This model uses areal-referenced basis function expansions. One areal-referenced basis function to use is the Moran's I basis functions (Bradley et al., 2015; Bradley et al., 2018) or the Obled-Creutin basis functions (Bradley et al., 2017; Obled & Creutin, 1986), which have been used in a multivariate multiscale framework (Daw et al., 2022). In the bivariate case, we consider an ordered hierarchical model and use basis functions to model one of the variables. Ordering variables may be very difficult in such models, but is straightforward for bivariate data (Banerjee et al., 2015, pg. 274). We also consider the MCAR model (Carlin & Banerjee, 2003; Gelfand & Vounatsou, 2003). As an extension of the CAR model, the MCAR model is naturally defined for areal data and adopts a separable-type structure using the Kronecker product in the covariance specification for computational gains (Mardia & Goodall, 1993).

In this paper, we propose three bivariate multiscale spatial models by combining the

multivariate spatial random effects model, MCAR model, and ordered hierarchical model with the multiscale spatial approach within a Bayesian hierarchical modeling framework. Bayesian modeling is fairly natural for our application, since our data is particularly high-dimensional and Bayesian modeling allows for uncertainty quantification. We call these models the multiscale spatial random effects (MS-SRE) model, the multiscale MCAR (MS-MCAR) model, and the multiscale ordered hierarchical (MS-OH) model. All three strategies, namely, MS-SRE, MS-MCAR, and MS-OH are new (i.e., to our knowledge have not been formally introduced in the literature), and they each represent a contribution.

Our work not only presents multiple new bivariate multiscale spatial models but also provides a comparison of these new models based on their prediction performance and computational efficiency. We conduct an extensive simulation study and demonstrate the efficiency of our models through real data analysis. The remainder of this paper will be organized as follows. In Section 2, we will review the three single-scale bivariate spatial models along with the multiscale approach. Section 3 gives the methodologies for combining the bivariate spatial models with the multiscale approach, and presents Bayesian hierarchical model specifications for all the three combinations we investigate. Section 4 consists of a simulation study that compares the three proposed models for bivariate multiscale data. We analyze data obtained from the Dartmouth Atlas Study in Section 5. A discussion in Section 6 then follows to conclude this paper. Derivations of full-conditional distributions are provided in Appendix A.

2 Preliminaries

In this section, we review single-scale bivariate spatial models (Section 2.1) and an univariate multiscale approach (Section 2.2).

2.1 Review: Single-scale bivariate spatial models

In this review, we consider a bivariate and intercept-only setting. Suppose we observe $\{Y_1(A_1), \dots, Y_1(A_n), Y_2(A_1), \dots, Y_2(A_n)\}$, where $Y_j(A_i)$ denotes the j -th variable observed on i -th areal unit for variables/processes $j = 1, 2$ and $i = 1, \dots, n$. Here $A_i \subset D$ where $D \subset \mathbb{R}^d$ is the spatial domain of interest. For ease of exposition, we specify types of spatial random effects (SRE), multivariate conditional autoregressive (MCAR), and ordered hierarchical (OH) models in Table 1.

In the SRE model, the basis functions $\mathbf{g}(A_i)$ are chosen to be the r -dimensional Moran's I basis functions as defined in Bradley et al. (2015) and Hughes & Haran (2013). In particular, we set $\mathbf{g}(A_i)$ equal to the first r eigenvectors of the Moran's I operator (Moran, 1950). The Moran's I operator, denoted $\mathbf{M}(\mathbf{W})$, has the following form

$$\mathbf{M}(\mathbf{W}) = (\mathbf{I}_n - \mathbf{1}_n(\mathbf{1}'_n \mathbf{1}_n)^{-1} \mathbf{1}'_n) \mathbf{W} (\mathbf{I}_n - \mathbf{1}_n(\mathbf{1}'_n \mathbf{1}_n)^{-1} \mathbf{1}'_n)$$

where \mathbf{I}_n is the $n \times n$ identity matrix, $\mathbf{1}_n$ is the n -dimensional vector of all ones for the intercept-only setting, and \mathbf{W} is the $n \times n$ adjacency matrix defined by areal units $\{A_1, \dots, A_n\}$. The (i, j) -th entry of the adjacency matrix \mathbf{W} is 1 if A_i is a neighbor of A_j ,

	SRE model	MCAR model	OH model
DM 1	$Y_1(A_i) \beta_1, \boldsymbol{\eta}, \sigma_1^2 \stackrel{i.i.d.}{\sim} N(\beta_1 + \mathbf{g}_1(A_i)' \boldsymbol{\eta}, \sigma_1^2)$	$Y_1(A_i) \beta_1, \boldsymbol{\psi}, \sigma_1^2 \stackrel{i.i.d.}{\sim} N(\beta_1 + \psi_{1i}, \sigma_1^2)$	$Y_1(A_i) \beta_1, \boldsymbol{\eta}, \sigma_1^2 \stackrel{i.i.d.}{\sim} N(\beta_1 + \mathbf{g}_1(A_i)' \boldsymbol{\eta}, \sigma_1^2)$
DM 2	$Y_2(A_i) \beta_2, \boldsymbol{\eta}, \sigma_2^2 \stackrel{i.i.d.}{\sim} N(\beta_2 + \mathbf{g}_2(A_i)' \boldsymbol{\eta}, \sigma_2^2)$	$Y_2(A_i) \beta_2, \boldsymbol{\psi}, \sigma_2^2 \stackrel{i.i.d.}{\sim} N(\beta_2 + \psi_{2i}, \sigma_2^2)$	$Y_2(A_i) \beta_0, \beta_1, \beta_2, \boldsymbol{\eta}, \sigma_2^2 \stackrel{i.i.d.}{\sim} N(\beta_0 + \beta_2(\beta_1 + \mathbf{g}_1(A_i)' \boldsymbol{\eta}), \sigma_2^2)$
PrM	$\boldsymbol{\eta} \sigma_\eta^2, \phi \sim MVN(\mathbf{0}, \mathbf{K})$ where $\mathbf{K} = \{\sigma_\eta^2 \exp(-\phi \ \mathbf{c}_i - \mathbf{c}_j\)\}$	$\boldsymbol{\psi} \rho, \tau, \nu^2 \sim MVN(\mathbf{0}, \boldsymbol{\Sigma} \otimes (\mathbf{D} - \rho \mathbf{W})^{-1})$ where $\boldsymbol{\Sigma} = \nu^2 \mathbf{T}(\tau)$	$\boldsymbol{\eta} \sigma_\eta^2, \phi \sim MVN(\mathbf{0}, \mathbf{K})$ where $\mathbf{K} = \{\sigma_\eta^2 \exp(-\phi \ \mathbf{c}_i - \mathbf{c}_j\)\}$
PM 1	$\beta_k \stackrel{i.i.d.}{\sim} N(0, \sigma_\beta^2)$ for $k = 1, 2$	$\beta_k \stackrel{i.i.d.}{\sim} N(0, \sigma_\beta^2)$ for $k = 1, 2$	$\beta_k \stackrel{i.i.d.}{\sim} N(0, \sigma_\beta^2)$ for $k = 0, 1, 2$
PM 2	$\sigma_\eta^2 \sim IG(a_\eta, b_\eta)$	$\nu^2 \sim IG(a_\nu, b_\nu)$	$\sigma_\eta^2 \sim IG(a_\eta, b_\eta)$
PM 3	$\sigma_k^2 \stackrel{i.i.d.}{\sim} IG(a_\sigma, b_\sigma)$ for $k = 1, 2$	$\sigma_k^2 \stackrel{i.i.d.}{\sim} IG(a_\sigma, b_\sigma)$ for $k = 1, 2$	$\sigma_k^2 \stackrel{i.i.d.}{\sim} IG(a_\sigma, b_\sigma)$ for $k = 1, 2$
PM 4	$\phi \sim Unif(a_\phi, b_\phi)$	$\rho \sim Unif(a_\rho, b_\rho)$	$\phi \sim Unif(a_\phi, b_\phi)$
PM 5	—	$\tau \sim Unif(a_\tau, b_\tau)$	—

Table 1: Single-scale bivariate spatial models. Here DM, PrM, and PM are abbreviations for the data model, process model, and parameter model, respectively. Let $N(\mu, \sigma^2)$ be the univariate normal distribution with mean μ and variance σ^2 , and $MVN(\boldsymbol{\mu}, \boldsymbol{\Sigma})$ be the multivariate normal distribution with vector mean $\boldsymbol{\mu}$ and covariance matrix $\boldsymbol{\Sigma}$. Let IG and $Unif$ be the inverse gamma and uniform distributions, respectively. Let $\mathbf{g} : \{A_1, \dots, A_n\} \rightarrow \mathbb{R}^r$ be an r -dimensional vector of basis functions.

and is 0 if it is not. Using the spectral decomposition $\mathbf{M}(\mathbf{W}) = \boldsymbol{\Phi} \boldsymbol{\Lambda} \boldsymbol{\Phi}'$, we can specify $\mathbf{G} = (\mathbf{g}(A_1)', \dots, \mathbf{g}(A_n)')'$ to be the first r columns of $\boldsymbol{\Phi}$. It has been shown recently (Khan & Calder, 2022) that the Moran’s I basis can lead to simplistic estimates for the regression effects, and lead to reasonable predictions. Since the goal of COS is prediction, Moran’s I basis is reasonable to use here. In the multiscale space-time COS literature, it has been demonstrated (Raim et al., 2021) that the choice $\mathbf{K} = cov(\boldsymbol{\eta})$ leads to little-to-no impact on prediction, which is our primary inferential goal. As such, we choose a simple structure for \mathbf{K} . In particular, the $r \times r$ covariance matrix $\mathbf{K} = \{\sigma_\eta^2 \exp(-\phi \|\mathbf{c}_i - \mathbf{c}_j\|)\}$, where $\{\mathbf{c}_1, \mathbf{c}_2, \dots, \mathbf{c}_r\} \in D$ are the prespecified knots (Banerjee et al., 2008). Of course, there are several alternative options that have been used in the past, including but not limited to Obled-Creutin basis functions for $\mathbf{g}(\cdot)$ (Bradley et al., 2017; Obled & Creutin, 1986), and inverse Wishart distribution for \mathbf{K} , among others.

We also use basis functions for the first response variable in the OH model (Messick et al., 2017). The choice of basis functions and priors for the parameters are identical to those in the SRE model. The key difference is that the dependence between variables is not induced through a shared random vector like in the SRE model but through a hierarchy structure in the data models. Specifically, $Y_2(A_i)$ in the OH model is assumed a mean that is a scaled version of the mean of $Y_1(A_i)$ (i.e., $\beta_0 + \beta_2(\beta_1 + \mathbf{g}_1(A_i)' \boldsymbol{\eta})$).

In the MCAR model, $\boldsymbol{\psi} = (\psi_{11}, \dots, \psi_{1n}, \psi_{21}, \dots, \psi_{2n})'$ is assumed a multivariate normal process with mean zero and covariance $\boldsymbol{\Sigma} \otimes (\mathbf{D} - \rho \mathbf{W})^{-1}$, where \mathbf{W} is the adjacency matrix for areal units $\{A_1, \dots, A_n\}$, $\mathbf{D} = diag(w_{i+} : i = 1, \dots, n)$ where w_{i+} is the sum of all the elements in row i of \mathbf{W} , ρ is an unknown scalar, and $\boldsymbol{\Sigma}$ is a 2×2 covariance matrix. The symbol “ \otimes ” denotes the Kronecker product that combines the spatial dependence and the nonspatial correlation between the two variables. The matrix $\boldsymbol{\Sigma}$ is usually given an inverse Wishart prior (Banerjee et al., 2015). However, this can be simplified in bivariate setting by letting $\boldsymbol{\Sigma} = \nu^2 \mathbf{T}(\tau)$, where the scalar ν^2 gives the variance and $\mathbf{T}(\tau)$ is a 2×2 matrix with one on the diagonal and correlation parameter τ everywhere else. This specification greatly speeds up the computation since it now only requires updating two unknowns instead of four unknowns.

2.2 A review of a multiscale approach

We consider a multiscale approach for spatial data observed at more than one areal scale. Suppose we observe data at two different areal scales, denoted $\mathbf{Y}_B = (Y(B_1), Y(B_2), \dots, Y(B_{n_b}))'$ where $B_i \in D_B$, $B_i \subset \mathbb{R}^d$, $D_B = \{B_1, \dots, B_{n_b}\}$ and $\mathbf{Y}_C = (Y(C_1), Y(C_2), \dots, Y(C_{n_c}))'$ where $C_j \in D_C$, $C_j \subset \mathbb{R}^d$, $D_C = \{C_1, \dots, C_{n_c}\}$. The two areal supports are spatially misaligned, and B_i and C_j may or may not overlap with each other for all $i = 1, \dots, n_b$ and $j = 1, \dots, n_c$. For example, B_i could represent a hospital service area (HSA), while C_j could represent a county. Our inferential goal is to predict $\mathbf{Y}_A = (Y(A_1), Y(A_2), \dots, Y(A_{n_a}))'$ where $A_l \in D_A$, $A_l \subset \mathbb{R}^d$, and $D_A = \{A_1, \dots, A_{n_a}\}$ where $n_a \geq \max\{n_b, n_c\}$. The target support D_A is another areal scale given by the partitioning of D_B and D_C . We call D_A the “partition scale.” Figure 1 demonstrates the partitioning for such sets of regions. In this demonstration, we let $n_b = 4$ and $n_c = 2$. The resulting partition scale D_A has $n_a = 9$ areal units. The multiscale approach assumes the process is piece-wise constant over D_A . Then, we can write \mathbf{Y}_B and \mathbf{Y}_C as follows,

$$\mathbf{Y}_B = \left(Y(A_1), \frac{|A_2|Y(A_2) + |A_3|Y(A_3)}{|A_2 \cup A_3|}, \frac{|A_4|Y(A_4) + |A_7|Y(A_7)}{|A_4 \cup A_7|}, \frac{|A_5|Y(A_5) + |A_6|Y(A_6)}{|A_5 \cup A_6|} \right)' \quad (1)$$

$$\mathbf{Y}_C = \left(\frac{|A_3|Y(A_3) + |A_4|Y(A_4) + |A_5|Y(A_5) + |A_8|Y(A_8)}{|A_3 \cup A_4 \cup A_5 \cup A_8|}, Y(A_9) \right)',$$

where $|\cdot|$ denotes the area of the region. By assuming a spatial model on \mathbf{Y}_A , we can define data models for \mathbf{Y}_B and \mathbf{Y}_C based on (1).

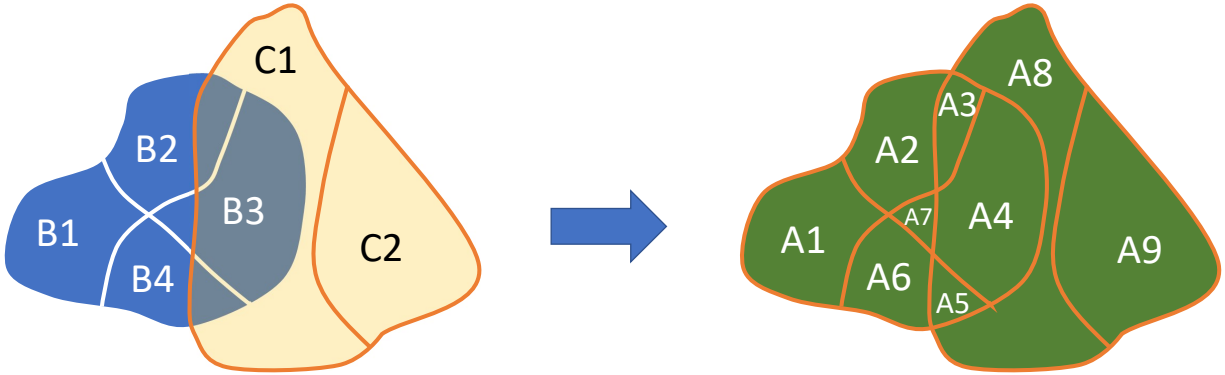


Figure 1: Partitioning plot of multiscale areal units. In the left panel the blue regions represent D_B and the yellow regions represent D_C . The green regions represent D_A , which consists of the regions formed by partitioning D_B and D_C .

3 Methodologies

In this section, we introduce the three bivariate multiscale spatial models. Section 3.1 describes the way to combine bivariate spatial models with the multiscale approach, and

Section 3.2 provides detailed model specifications for all three bivariate multiscale spatial models.

3.1 Combining SRE, MCAR, and OH models with the multiscale approach

For bivariate spatial data observed at misaligned areal supports, we consider combining the SRE, MCAR, and OH models with the multiscale approach. We refer to the combined models as the multiscale spatial random effects (MS-SRE) model, the multiscale MCAR (MS-MCAR) model, and the multiscale ordered hierarchical (MS-OH) model. Suppose we observe $\mathbf{Y}_1 = (Y_1(B_1), \dots, Y_1(B_{n_1}))'$ where $B_i \in D_1$, $B_i \subset \mathbb{R}^d$, $D_1 = \{B_1, \dots, B_{n_1}\}$ and $\mathbf{Y}_2 = (Y_2(C_1), \dots, Y_2(C_{n_2}))'$ where $C_j \in D_2$, $C_j \subset \mathbb{R}^d$, $D_2 = \{C_1, \dots, C_{n_2}\}$. Our inferential goal is to predict both variables at another areal scale that is the partition of D_1 and D_2 . We denote this partitioned areal scale as D_A with areal units $\{A_l : l = 1, \dots, n_3\}$ where $A_l \subset \mathbb{R}^d$. Analogous to (1), we can write $Y_1(B_i)$ and $Y_2(C_j)$ in terms of $Y_1(A_l)$ and $Y_2(A_l)$ respectively, so that assuming a bivariate spatial model on $\mathbf{Y}_A = (Y_1(A_1), \dots, Y_1(A_{n_3}), Y_2(A_1), \dots, Y_2(A_{n_3}))'$ would naturally produce data models for \mathbf{Y}_1 and \mathbf{Y}_2 .

We arrange the redefined $Y_1(B_i)$ and $Y_2(C_j)$ in matrix form. Let us define \mathbf{Y}_A into two vectors, $\mathbf{Y}_{A1} = (Y_1(A_1), \dots, Y_1(A_{n_3}))'$ and $\mathbf{Y}_{A2} = (Y_2(A_1), \dots, Y_2(A_{n_3}))'$. We can write $\mathbf{Y}_1 = \mathbf{P}_1 \mathbf{Y}_{A1}$ and $\mathbf{Y}_2 = \mathbf{P}_2 \mathbf{Y}_{A2}$ based on the partition. We refer to the $n_1 \times n_3$ matrix \mathbf{P}_1 and $n_2 \times n_3$ matrix \mathbf{P}_2 as partition matrices. The partition matrices \mathbf{P}_1 and \mathbf{P}_2 can be explicitly defined as

$$\mathbf{P}_1 = \begin{pmatrix} \frac{|A_1|}{|B_1|} I(A_1 \subset B_1) & \frac{|A_2|}{|B_1|} I(A_2 \subset B_1) & \cdots & \frac{|A_{n_3}|}{|B_1|} I(A_{n_3} \subset B_1) \\ \frac{|A_1|}{|B_2|} I(A_1 \subset B_2) & \frac{|A_2|}{|B_2|} I(A_2 \subset B_2) & \cdots & \frac{|A_{n_3}|}{|B_2|} I(A_{n_3} \subset B_2) \\ \vdots & \ddots & & \vdots \\ \frac{|A_1|}{|B_{n_1}|} I(A_1 \subset B_{n_1}) & \frac{|A_2|}{|B_{n_1}|} I(A_2 \subset B_{n_1}) & \cdots & \frac{|A_{n_3}|}{|B_{n_1}|} I(A_{n_3} \subset B_{n_1}) \end{pmatrix}$$

$$\mathbf{P}_2 = \begin{pmatrix} \frac{|A_1|}{|C_1|} I(A_1 \subset C_1) & \frac{|A_2|}{|C_1|} I(A_2 \subset C_1) & \cdots & \frac{|A_{n_3}|}{|C_1|} I(A_{n_3} \subset C_1) \\ \frac{|A_1|}{|C_2|} I(A_1 \subset C_2) & \frac{|A_2|}{|C_2|} I(A_2 \subset C_2) & \cdots & \frac{|A_{n_3}|}{|C_2|} I(A_{n_3} \subset C_2) \\ \vdots & \ddots & & \vdots \\ \frac{|A_1|}{|C_{n_2}|} I(A_1 \subset C_{n_2}) & \frac{|A_2|}{|C_{n_2}|} I(A_2 \subset C_{n_2}) & \cdots & \frac{|A_{n_3}|}{|C_{n_2}|} I(A_{n_3} \subset C_{n_2}) \end{pmatrix},$$

respectively, where $I(\cdot)$ is an indicator function. Putting together \mathbf{Y}_1 and \mathbf{Y}_2 , we have

$$\mathbf{Y} = \begin{pmatrix} \mathbf{Y}_1 \\ \mathbf{Y}_2 \end{pmatrix} = \begin{pmatrix} \mathbf{P}_1 \mathbf{Y}_{A1} \\ \mathbf{P}_2 \mathbf{Y}_{A2} \end{pmatrix} = \begin{pmatrix} \mathbf{P}_1 & \mathbf{0} \\ \mathbf{0} & \mathbf{P}_2 \end{pmatrix} \mathbf{Y}_A = \mathbf{P} \mathbf{Y}_A \quad (2)$$

where \mathbf{P} has dimension $(n_1 + n_2) \times 2n_3$. Assuming bivariate spatial SRE, MCAR, and OH models on \mathbf{Y}_A , we can build corresponding data models (DM) for \mathbf{Y} through the predictive distribution (PD) for \mathbf{Y}_A in (2).

For illustration, we provide the PD for \mathbf{Y}_{A1} and \mathbf{Y}_{A2} in the case of MS-SRE, and show how the PD induces a DM (i.e., the DM is a consequence of averaging the PD over the partitioning). A summary of the remaining multiscale models can be found in Table 2. The

PD for \mathbf{Y}_A assuming a SRE is,

$$\begin{aligned} \text{MS-SRE PD1} : \mathbf{Y}_{A1} | \beta_1, \boldsymbol{\eta}, \sigma_1^2 &\sim \text{MVN}(\beta_1 \mathbf{1}_{n_3} + \mathbf{G}_1 \boldsymbol{\eta}, \sigma_1^2 \mathbf{I}_{n_3}) \\ \text{MS-SRE PD2} : \mathbf{Y}_{A2} | \beta_2, \boldsymbol{\eta}, \sigma_2^2 &\sim \text{MVN}(\beta_2 \mathbf{1}_{n_3} + \mathbf{G}_2 \boldsymbol{\eta}, \sigma_2^2 \mathbf{I}_{n_3}), \end{aligned} \quad (3)$$

where $\mathbf{1}_{n_3}$ is an n_3 -dimensional vector of all ones, \mathbf{I}_{n_3} is an $n_3 \times n_3$ identity matrix, and the $n_3 \times r$ dimensional matrices $\mathbf{G}_1 = (\mathbf{g}_1(A_1)', \dots, \mathbf{g}_1(A_{n_3})')'$ and $\mathbf{G}_2 = (\mathbf{g}_2(A_1)', \dots, \mathbf{g}_2(A_{n_3})')'$ are spatial basis functions. Equation (3) is simply the DM1 and DM2 from a bivariate SRE model in Table 1, applied to the predictive data \mathbf{Y}_{A1} and \mathbf{Y}_{A2} . Based on (2) and (3), we can achieve data models for our observed \mathbf{Y}_1 and \mathbf{Y}_2 defined on $\{B_i\}$ and $\{C_j\}$:

$$\begin{aligned} \text{MS-SRE DM1} : \mathbf{Y}_1 | \beta_1, \boldsymbol{\eta}, \sigma_1^2 &\sim \text{MVN}(\beta_1 \mathbf{1}_{n_1} + \mathbf{P}_1 \mathbf{G}_1 \boldsymbol{\eta}, \sigma_1^2 \mathbf{P}_1 \mathbf{P}_1') \\ &\text{or } Y_1(B_i) | \beta_1, \boldsymbol{\eta}, \sigma_1^2 \stackrel{\text{ind}}{\sim} N(\beta_1 + \mathbf{g}_1(B_i)' \boldsymbol{\eta}, \sigma_1^2 (\mathbf{P}_1 \mathbf{P}_1')_{ii}) \\ \text{MS-SRE DM2} : \mathbf{Y}_2 | \beta_2, \boldsymbol{\eta}, \sigma_2^2 &\sim \text{MVN}(\beta_2 \mathbf{1}_{n_2} + \mathbf{P}_2 \mathbf{G}_2 \boldsymbol{\eta}, \sigma_2^2 \mathbf{P}_2 \mathbf{P}_2') \\ &\text{or } Y_2(C_j) | \beta_2, \boldsymbol{\eta}, \sigma_2^2 \stackrel{\text{ind}}{\sim} N(\beta_2 + \mathbf{g}_2(C_j)' \boldsymbol{\eta}, \sigma_2^2 (\mathbf{P}_2 \mathbf{P}_2')_{jj}). \end{aligned} \quad (4)$$

The scalar forms are also provided, where the r -dimensional vector $\mathbf{g}_1(B_i)'$ ($\mathbf{g}_2(C_j)'$) corresponds to the $i(j)$ -th row of the $n_1 \times r$ ($n_2 \times r$) matrix $\mathbf{P}_1 \mathbf{G}_1$ ($\mathbf{P}_2 \mathbf{G}_2$), and $(\mathbf{P}_1 \mathbf{P}_1')_{ii}$ ($(\mathbf{P}_2 \mathbf{P}_2')_{jj}$) denotes the $i(j)$ -th diagonal element of the matrix $\mathbf{P}_1 \mathbf{P}_1'$ ($\mathbf{P}_2 \mathbf{P}_2'$). Notice that for disjoint set $\{B_i; i = 1, \dots, n_1\}$ (or $\{C_j; j = 1, \dots, n_2\}$) each column of \mathbf{P}_1 (or \mathbf{P}_2) would have at most one nonzero element since a partitioned unit cannot belong to more than one B_i (or C_j). Therefore, $\mathbf{P}_1 \mathbf{P}_1'$ and $\mathbf{P}_2 \mathbf{P}_2'$ are diagonal matrices, which makes writing the data models in scalar form easy.

3.2 Markov Chain Monte Carlo specifications

We summarize MS-SRE, MS-MCAR, MS-OH models in Table 2. To implement these three models, we adopt the Metropolis-within-Gibbs Markov Chain Monte Carlo (MCMC) algorithm to sample from the posterior. Relatively flat priors are given for all of the parameters in these models. Specifications of the hyperparameters will be deferred to Section 4. The update of ϕ (in MS-SRE and MS-OH models), ρ , and τ (in MS-MCAR model) require Metropolis-Hastings steps. For the simulation study in Section 4, the three new models will be compared based on prediction performance and computational efficiency. We will generate 5,000 samples and discard the first 1,000 as burn-in for simulation. The models are implemented for the analysis of the Texas blood test monitoring data obtained from the Dartmouth Atlas Study in Section 5, where 10,000 samples will be generated with the first 2,000 discarded for burn-in.

4 Simulation

We consider bivariate multiscale spatial data observed on two misaligned areal supports. We let the first areal support D_1 be a regular 10×10 grid on the unit square $[0, 1] \times [0, 1]$. We consider the second areal support D_2 to consist of 225 irregular regions whose union also gives the unit square. We describe the construction of D_1 and D_2 in Figure 2. In the

	Bayesian Hierarchical Models	COS Prediction
MS-SRE	$DM1 : Y_1(B_i) \beta_1, \boldsymbol{\eta}, \sigma_1^2 \stackrel{i.i.d.}{\sim} N(\beta_1 + \mathbf{g}_1(B_i)' \boldsymbol{\eta}, \sigma_1^2 (\mathbf{P}_1 \mathbf{P}_1')_{ii})$	$Y_1(A_t) \beta_1, \boldsymbol{\eta}, \sigma_1^2 \stackrel{i.i.d.}{\sim} N(\beta_1 + \mathbf{g}_1(A_t)' \boldsymbol{\eta}, \sigma_1^2)$
	$DM2 : Y_2(C_j) \beta_2, \boldsymbol{\eta}, \sigma_2^2 \stackrel{i.i.d.}{\sim} N(\beta_2 + \mathbf{g}_2(C_j)' \boldsymbol{\eta}, \sigma_2^2 (\mathbf{P}_2 \mathbf{P}_2')_{jj})$	$Y_2(A_t) \beta_2, \boldsymbol{\eta}, \sigma_2^2 \stackrel{i.i.d.}{\sim} N(\beta_2 + \mathbf{g}_2(A_t)' \boldsymbol{\eta}, \sigma_2^2)$
	$PrM : \boldsymbol{\eta} \sigma_\eta^2, \phi \sim MVN(\mathbf{0}, \mathbf{K})$ where $\mathbf{K} = \{\sigma_\eta^2 \exp(-\phi \ \mathbf{c}_i - \mathbf{c}_j\)\}$	
	$PM1 : \beta_k \stackrel{i.i.d.}{\sim} N(0, \sigma_\beta^2) \text{ for } k = 1, 2$ $PM2 : \sigma_\eta^2 \sim IG(a_\eta, b_\eta)$ $PM3 : \sigma_k^2 \stackrel{i.i.d.}{\sim} IG(a_\sigma, b_\sigma) \text{ for } k = 1, 2$ $PM4 : \phi \sim Unif(a_\phi, b_\phi)$	
MS-MCAR	$DM1 : Y_1(B_i) \beta_1, \boldsymbol{\psi}, \sigma_1^2 \stackrel{i.i.d.}{\sim} N(\beta_1 + \mathbf{p}(B_i)' \boldsymbol{\psi}, \sigma_1^2 (\mathbf{P}_1 \mathbf{P}_1')_{ii})$	$Y_1(A_t) \beta_1, \boldsymbol{\psi}, \sigma_1^2 \stackrel{i.i.d.}{\sim} N(\beta_1 + \psi_{1t}, \sigma_1^2)$
	$DM2 : Y_2(C_j) \beta_2, \boldsymbol{\psi}, \sigma_2^2 \stackrel{i.i.d.}{\sim} N(\beta_2 + \mathbf{p}(C_j)' \boldsymbol{\psi}, \sigma_2^2 (\mathbf{P}_2 \mathbf{P}_2')_{jj})$	$Y_2(A_t) \beta_2, \boldsymbol{\psi}, \sigma_2^2 \stackrel{i.i.d.}{\sim} N(\beta_2 + \psi_{2t}, \sigma_2^2)$
	$PrM : \boldsymbol{\psi} \rho, \tau, \nu^2 \sim MVN(\mathbf{0}, \boldsymbol{\Sigma} \otimes (\mathbf{D} - \rho \mathbf{W})^{-1})$ where $\boldsymbol{\Sigma} = \nu^2 \mathbf{T}(\boldsymbol{\tau})$	
	$PM1 : \beta_k \stackrel{i.i.d.}{\sim} N(0, \sigma_\beta^2) \text{ for } k = 1, 2$ $PM2 : \rho \sim Unif(a_\rho, b_\rho)$ $PM3 : \tau \sim Unif(a_\tau, b_\tau)$ $PM4 : \nu^2 \sim IG(a_\nu, b_\nu)$ $PM5 : \sigma_k^2 \stackrel{i.i.d.}{\sim} IG(a_\sigma, b_\sigma) \text{ for } k = 1, 2$	
MS-OH	$DM1 : Y_1(B_i) \beta_1, \boldsymbol{\eta}, \sigma_1^2 \stackrel{i.i.d.}{\sim} N(\beta_1 + \mathbf{g}_1(B_i)' \boldsymbol{\eta}, \sigma_1^2 (\mathbf{P}_1 \mathbf{P}_1')_{ii})$	$Y_1(A_t) \beta_1, \boldsymbol{\eta}, \sigma_1^2 \stackrel{i.i.d.}{\sim} N(\beta_1 + \mathbf{g}_1(A_t)' \boldsymbol{\eta}, \sigma_1^2)$
	$DM2 : Y_2(C_j) \beta_0, \beta_1, \beta_2, \boldsymbol{\eta}, \sigma_2^2 \stackrel{i.i.d.}{\sim} N(\beta_0 + \beta_2(\beta_1 + \mathbf{g}_1(C_j)' \boldsymbol{\eta}), \sigma_2^2 (\mathbf{P}_2 \mathbf{P}_2')_{jj})$	$Y_2(A_t) \beta_0, \beta_1, \beta_2, \boldsymbol{\eta}, \sigma_2^2 \stackrel{i.i.d.}{\sim} N(\beta_0 + \beta_2(\beta_1 + \mathbf{g}_1(A_t)' \boldsymbol{\eta}), \sigma_2^2)$
	$PrM : \boldsymbol{\eta} \sigma_\eta^2, \phi \sim MVN(\mathbf{0}, \mathbf{K})$ where $\mathbf{K} = \{\sigma_\eta^2 \exp(-\phi \ \mathbf{c}_i - \mathbf{c}_j\)\}$	
	$PM1 : \beta_k \stackrel{i.i.d.}{\sim} N(0, \sigma_\beta^2) \text{ for } k = 0, 1, 2$ $PM2 : \sigma_\eta^2 \sim IG(a_\eta, b_\eta)$ $PM3 : \sigma_k^2 \stackrel{i.i.d.}{\sim} IG(a_\sigma, b_\sigma) \text{ for } k = 1, 2$ $PM4 : \phi \sim Unif(a_\phi, b_\phi)$	

Table 2: Multiscale bivariate spatial models. Here DM, PrM, and PM are abbreviations for the data model, process model, and parameter model, respectively. Let $N(\mu, \sigma^2)$ be the univariate normal distribution with mean μ and variance σ^2 , and $MVN(\boldsymbol{\mu}, \boldsymbol{\Sigma})$ be the multivariate normal distribution with vector mean $\boldsymbol{\mu}$ and covariance matrix $\boldsymbol{\Sigma}$. Let IG and $Unif$ be the inverse gamma and uniform distributions, respectively. Let $\mathbf{p}(\cdot)'$ be the corresponding row in the partition matrix \mathbf{P} defined in (2).

first panel of the Figure 2, we plot B_1, B_2, B_3 , and B_4 ($\cup_{i=1}^4 B_i = [0, 0.2] \times [0, 0.2]$). The remaining B_i are defined according to a 10×10 grid over $[0, 1] \times [0, 1]$. The second panel contains C_1, \dots, C_9 ($\cup_{j=1}^9 C_j = [0, 0.2] \times [0, 0.2]$), which is irregular. The remaining C_j are defined by shifting C_1, \dots, C_9 . That is, stacking C_1, \dots, C_9 over five rows and five columns produces an irregular grid over $[0, 1] \times [0, 1]$ with 225 areal units. We choose the areal units in D_2 to have this irregular structure, as shown in Figure 2, such that its partition with D_1 would produce a 20×20 regular grid (denoted D_A) on the unit square. For each of the three Bayesian hierarchical models specified in Table 2, we want to generate $n_1 = 100$ number of observations for \mathbf{Y}_1 and $n_2 = 225$ number of observations for \mathbf{Y}_2 . Our goal is to obtain $n_3 = 400$ predictions for both variables on the target support D_A .

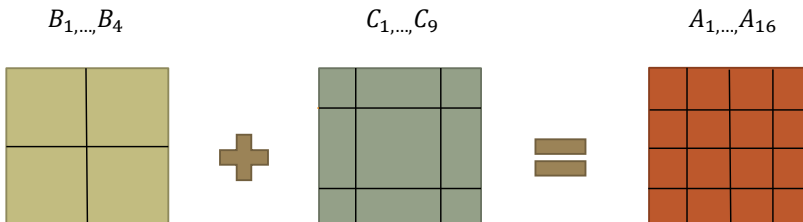


Figure 2: Illustration of the two areal supports D_1 and D_2 and their partition D_A over the subregion $[0, 0.2] \times [0, 0.2]$. In the first panel, we plot B_1, B_2, B_3 , and B_4 ($\cup_{i=1}^4 B_i = [0, 0.2] \times [0, 0.2]$). The remaining B_i are defined according to a 10×10 grid over $[0, 1] \times [0, 1]$. The second panel contains C_1, \dots, C_9 ($\cup_{j=1}^9 C_j = [0, 0.2] \times [0, 0.2]$), which is irregular. The remaining C_j are defined by shifting C_1, \dots, C_9 . That is, stacking C_1, \dots, C_9 over five rows and five columns produces an irregular grid over $[0, 1] \times [0, 1]$ with 225 areal units.

For the MS-SRE and MS-OH models, we select $r = 50$ equally spaced knots using the *cover.design* function in the R package *fields*. We choose $\sigma_\eta^2 = 1$ and $\phi = 0.1$ for the covariance \mathbf{K} of the random vector $\boldsymbol{\eta}$. In MS-SRE and MS-MCAR, we specify the constant mean to be $\beta_1 = 2$ and $\beta_2 = 5$. In MS-OH, we choose $\beta_0 = 0$, $\beta_1 = 2$, and $\beta_2 = 2$. The truth of σ_1^2 and σ_2^2 in all three models are chosen such that the signal to noise ratio is 5. In MS-MCAR, a true value for ρ close to one (i.e., $\rho = 0.9$) is necessary to produce realistic spatial association in the latent process (Banerjee et al., 2015, pg. 82). The variance and correlation parameters that make up the 2×2 matrix $\boldsymbol{\Sigma}$ are specified as $\nu^2 = 1.5$ and $\tau = 0.2$, respectively. The priors given to the parameters in all three models are considered relatively “flat” for a noninformative specification. Specifically, we have $\sigma_\beta^2 = 10^6$ and $a_\sigma = b_\sigma = a_\eta = b_\eta = a_\nu = b_\nu = 1$, which gives a prior variance of infinity. The parameter ϕ in the MS-SRE and MS-OH models is given a uniform prior with $a_\phi = 0$ and $b_\phi = 10$. The parameters ρ and τ in the MS-MCAR model are given uniform priors as well with $a_\rho = 0$, $b_\rho = 1$, $a_\tau = -1$, and $b_\tau = 1$, since in the bivariate case $|\rho| < 1$ (Banerjee et al., 2015, pg. 307).

We generate 20 datasets from each of the MS-SRE, MS-MCAR, and MS-OH models. For each simulated dataset, we fit all of the three models to it. No lack of convergence in the MCMC is detected through visually examining the trace plots. We compute the root mean square error (RMSE), $\sqrt{\frac{\sum_{i=1}^N (Y(A_i) - \hat{Y}(A_i))^2}{N}}$, for both variables on both their original

Variable	Scale	Truth	Fit:MS-SRE	Fit:MS-MCAR	Fit:MS-OH
Y_1	D_A	MS-SRE	0.073(0.040)	0.104(0.049)	0.093(0.038)
		MS-MCAR	0.543(0.027)	0.458(0.019)	0.552(0.029)
		MS-OH	0.149(0.062)	0.098(0.032)	0.094(0.038)
	D_1	MS-SRE	0.039(0.019)	0.069(0.026)	0.064(0.020)
		MS-MCAR	0.324(0.037)	0.161(0.026)	0.336(0.040)
		MS-OH	0.115(0.049)	0.035(0.003)	0.034(0.012)
Y_2	D_A	MS-SRE	0.074(0.042)	0.081(0.034)	0.077(0.042)
		MS-MCAR	0.525(0.024)	0.383(0.024)	0.507(0.028)
		MS-OH	0.213(0.092)	0.186(0.054)	0.182(0.074)
	D_2	MS-SRE	0.063(0.034)	0.065(0.033)	0.066(0.034)
		MS-MCAR	0.455(0.027)	0.232(0.033)	0.436(0.031)
		MS-OH	0.186(0.081)	0.128(0.025)	0.126(0.050)

Table 3: Simulation study results. The average(standard deviation) of RMSE by variable for multiscale models (MS-SRE, MS-MCAR, MS-OH) when the data is generated from different truths.

scales (i.e., D_1 or D_2) and the partition scale (i.e., D_A), and report the average and standard deviation of the RMSEs for the 20 datasets in Table 3. For each of the four blocks in the table, the bold numbers on the diagonal give the smallest average RMSEs for that corresponding row. This is expected since the model where the dataset is being generated should fit the data the best. For both variables, the RMSEs calculated for the inference scale D_A are always slightly larger than that for the original scale (i.e., D_1 and D_2). For the first variable, all three models perform relatively similarly when data is generated from the MS-SRE, compared to when data is generated from MS-MCAR or MS-OH. When MS-MCAR is the truth (i.e., the model where the data is being generated from), the average RMSEs are much larger in magnitude and the misspecified models have average RMSEs that are significantly larger (more than two standard deviations away). In the case when MS-OH is the truth, the average RMSE of MS-MCAR appears to be much closer to the average RMSE of MS-OH compared to that of MS-SRE. These results are consistent across different variables and scales.

We plot the prediction results for one simulated dataset from each model. The first column in Figures 3 and 4 shows the simulated Y_1 and Y_2 , respectively. For each of the two variables, the data are presented on the partition scale for comparison with the prediction plots. Recall we do not use the partition scale to fit our model, since in practice it is not observed, and the goal is to predict the process on the partition scale (i.e., COS). The prediction plots are shown in the remaining three columns of Figure 3 and Figure 4 for the first and second variable, respectively. Consistent with the results in Table 3, prediction plots 3c and 3d appear similar to each other. Spatial patterns shown in 3b can also be detected in these two prediction plots, suggesting that MS-MCAR and MS-OH perform similarly (although not as good) to MS-SRE when data is generated from MS-SRE. For data generated from MS-MCAR, all prediction plots 3f, 3g, and 3h seem to be relatively smooth; however, 3f and 3h are still less favorable compared to 3g. When comparing prediction plots

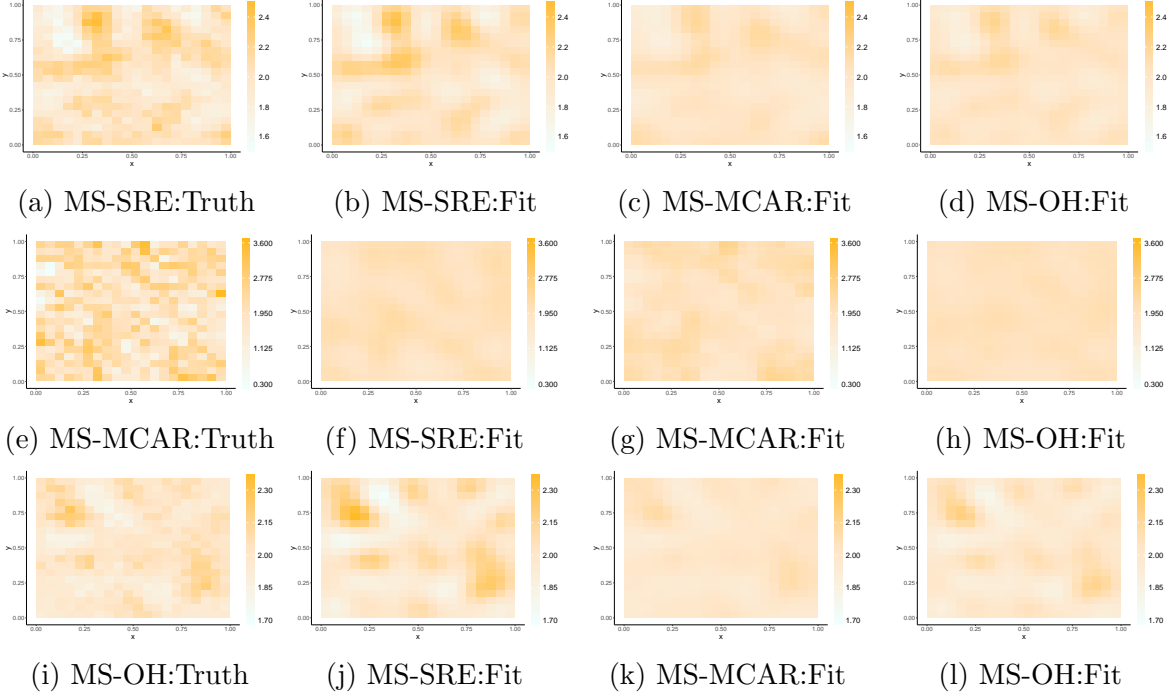


Figure 3: Data vs. prediction for Y_1 on D_A . The first column presents the simulated data on the partition scale D_A where each subcaption indicates the truth (i.e., from which model the data is simulated). The subsequent three columns give the predictions obtained by fitting the model indicated in the subcaption to the data with truth specified in the first plot of the corresponding row.

3j, 3k, and 3l to 3i, we see that MS-SRE overestimates large values when MS-OH is the truth, although this does not seem to hold for the second variable. Other conclusions made remain valid for Y_2 in Figure 4. Computationally, both MS-SRE and MS-OH outperform MS-MCAR in terms of efficiency. For fitting one simulated dataset with 5,000 iterations, the MS-SRE model needed 219.21 seconds to run, MS-OH model required 235.53 seconds, and MS-MCAR model required a much longer run-time of 9884.72 seconds.

5 Application

The Dartmouth Atlas Project reports health care data collected over United States annually. Specifically, they provide data on primary care access to determine the quality of hospitals within certain regions. Several quality measures are included and annual data are available on different areal scales. In our study, we are mainly interested in the blood test monitoring data used as hospital quality measures for Texas for the year 2015, and aim to jointly model the average annual percent of diabetic Medicare enrollees aged 65-75 having hemoglobin A1c test and average annual percent of diabetic Medicare enrollees aged 65-75 having blood lipids (LDL-C) test. These two tests are particularly important for senior diabetic patients, since they can be used to assess high blood sugar and high LDL-C (bad cholesterol) levels, which are known to be prevalent amongst diabetic patients

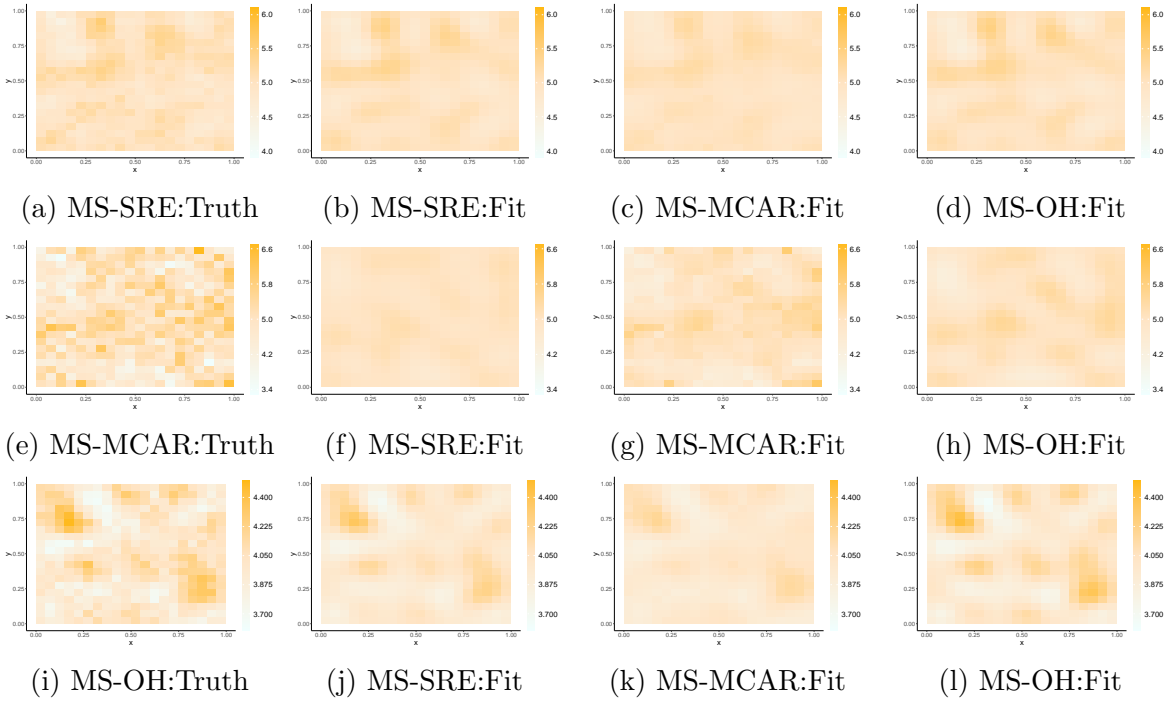


Figure 4: Data vs. prediction for Y_2 on D_A . The first column presents the simulated data on the partition scale D_A where each subcaption indicates the truth (i.e., from which model the data is simulated). The subsequent three columns give the predictions obtained by fitting the model indicated in the subcaption to the data with truth specified in the first plot of the corresponding row.

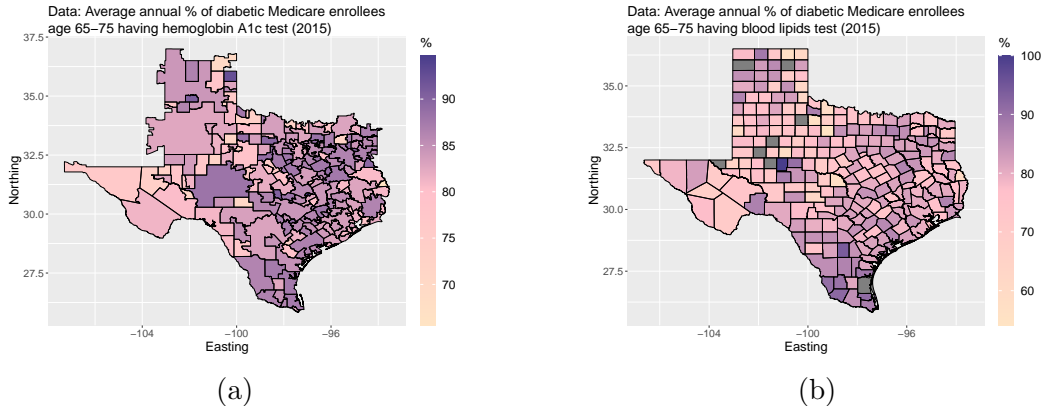


Figure 5: Texas blood test monitoring data in 2015. (a) Average annual percentage of diabetic Medicare enrollees age 65-75 having hemoglobin A1c test — observed on Texas hospital service areas (HSA). (b) Average annual percentage of diabetic Medicare enrollees age 65-75 having blood lipids test — observed on Texas counties.

(Habib & Aslam, 2003). We focus on age group 65-75, as this group is at higher risk for complications (Kirkman et al., 2012). Our bivariate multiscale models combine the first variable observed over Texas hospital service areas (HSA) with the second variable observed over Texas counties to produce higher resolution estimates of both variables.

We plot the data in Figure 5. Figure 5a shows the average annual percentage of diabetic Medicare enrollees aged 65-75 having hemoglobin A1c test by the 208 HSA. Notice that some of the HSA can go beyond the boundary of Texas. The eastern and southern regions appear to have higher response values (in purple), suggesting more diabetic patients taking the hemoglobin A1c test and thus better hospital quality there. Figure 5b illustrates the average annual percentage of diabetic Medicare enrollees aged 65-75 having blood lipids test over counties. The gray regions indicate the data is missing for that county. There are 254 counties in total in the state of Texas, out of which 246 counties have data observed. The data in Figure 5b appears smoother in the plot than that in Figure 5a. Nevertheless, the purple regions are mostly seen in the eastern and southern Texas as well.

Our inferential goal is to predict each variable on the partitioning formed by HSA and counties in Texas, which consists of 1,229 areal units in total. We fit the MS-SRE, MS-MCAR, and MS-OH models to the dataset and compare their prediction performance both through visually assessing the prediction plots and examining the widely applicable information criterion (WAIC, Watanabe, 2010). Again we choose $r = 150$ equally spaced knots for the models MS-SRE and MS-OH. The specifications of the hyperparameters for all three models are identical to those in the simulation study (see Section 4). The first 2,000 of 10,000 samples are discarded as burn-in, and the remaining 8,000 samples are used for analysis. Trace plots and Gelman-Rubin diagnostics (Gelman & Rubin, 1992) suggest that there is no issue with convergence.

The prediction plots are shown in Figure 6. The predictions in all six plots are given on the 1,229 partitioned units, with the first column showing the prediction for the average annual percentage of diabetic Medicare enrollees aged 65-75 having hemoglobin A1c test and the second column showing the prediction for the average annual percentage of diabetic

	Bivariate		Univariate	
	Y_1 (A1c test)	Y_2 (lipid test)	Y_1 (A1c test)	Y_2 (lipid test)
MS-SRE	-225.343	-269.240	-166.164	-215.343
MS-MCAR	-217.195	-299.990	-201.288	-281.975
MS-OH	-224.192	-266.550		

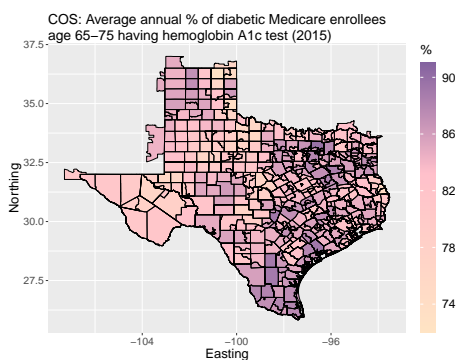
Table 4: Widely applicable information criterion (WAIC) for MS-SRE, MS-MCAR, and MS-OH. The column “bivariate” contains the WAIC when fitting our bivariate multiscale model, and the column “univariate” contains the WAIC when fitting the univariate multiscale model.

Medicare enrollees aged 65-75 having blood lipids test. The captions of the plots provide the name of the model from which the prediction is obtained. From the plot, all three models appear to perform similarly with similar spatial patterns in predictions. The WAIC reported in Table 4 shows that MS-SRE has the smallest WAIC for the A1c test and MS-MCAR has the smallest WAIC for the lipid test. Overall, MS-MCAR has the best prediction results considering the average of WAICs for both variables. We also compare the WAICs of bivariate COS with that of univariate COS. Note that the WAICs of univariate MS-OH are omitted in the table since MS-SRE and MS-OH are equivalent in the univariate case. For each of the three models, the bivariate WAIC for each variable is smaller than the corresponding univariate WAIC, as including the information of another variable would improve the prediction accuracy.

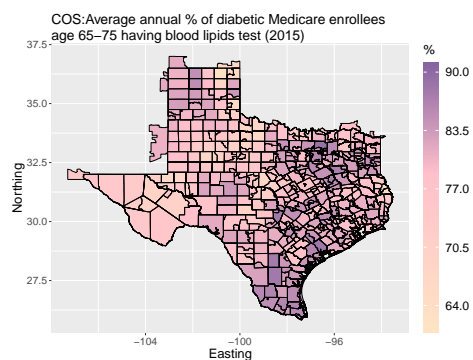
Our work is particularly important for those who are interested in making regulatory decisions (e.g., allocating funds for improvement in healthcare) based on hospital quality data such as blood tests. Our models allow us to obtain predictions at finer resolution, which can provide important insights that cannot be seen in the data observed on the original scale. For example, Figure 7 shows the difference between the data observed and the COS predictions obtained from MS-SRE for one HSA unit for the average annual percentage of diabetic Medicare enrollees aged 65-75 having A1c test. For illustration, we choose the HSA named San Antonio, whose location is highlighted in green in Figure 7a. Note that San Antonio is the name for this particular HSA, and hence, it has a border that is different from the border of the City of San Antonio, Texas (although two regions overlap). Figures 7b and 7c are segments of Figures 5a and 6a, respectively. The light purple color in Figure 7b suggests that San Antonio has a relatively high average annual percentage. However, from the finer resolution predictions in Figure 7c, we see that only one partitioning unit has a high predicted value.

6 Discussion

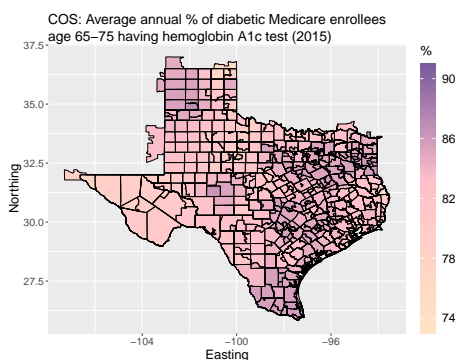
In this paper, we have developed three novel bivariate multiscale spatial models through combining several existing bivariate spatial models with a multiscale approach. Specifically, we present MS-SRE, MS-MCAR, and MS-OH for the multiscale data observed from two misaligned areal supports. We run a comprehensive simulation study to compare the three new models where we simulate data from two different areal supports and aim to predict on the partition of the two areal supports. We compare the RMSEs and prediction plots,



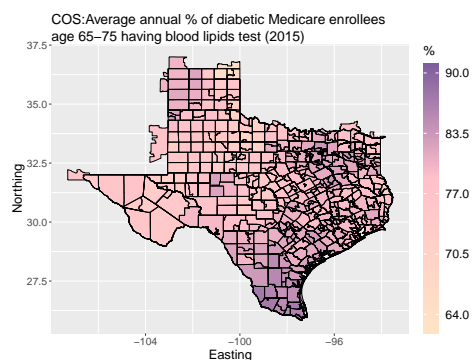
(a) MS-SRE



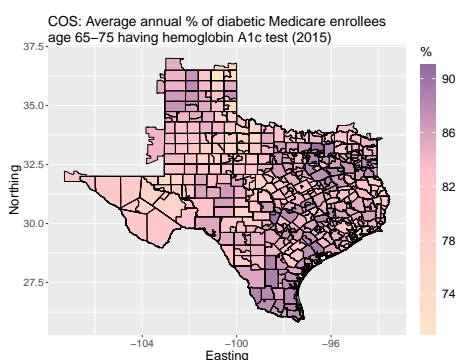
(b) MS-SRE



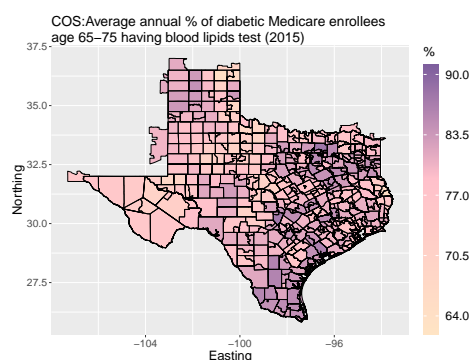
(c) MS-MCAR



(d) MS-MCAR



(e) MS-OH



(f) MS-OH

Figure 6: Prediction plots for Texas blood test monitoring data with captions indicating the model being fit. The first column gives predictions for average annual percentage of diabetic Medicare enrollees age 65-75 having hemoglobin A1c test. The second column gives predictions for average annual percentage of diabetic Medicare enrollees age 65-75 having blood lipids test. For both variables, the predictions from all three models are on the partition of HSA and counties of Texas.

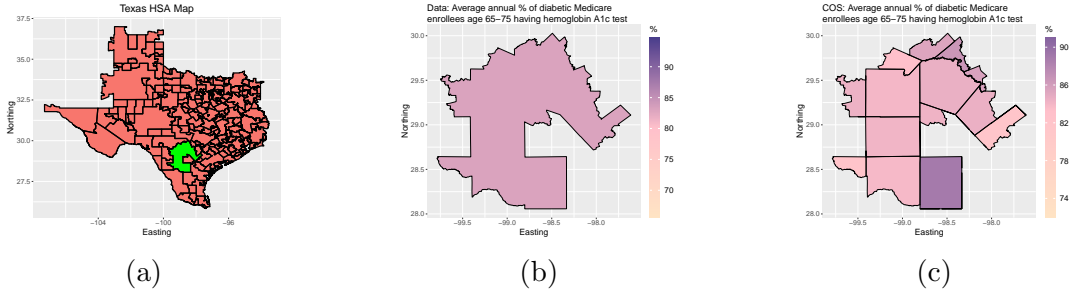


Figure 7: Observed data and COS prediction from MS-SRE for one HSA (i.e., San Antonio) (a) A map that shows all Texas HSA. The green region is the HSA named San Antonio. (b) Average annual percentage of diabetic Medicare enrollees age 65-75 having hemoglobin A1c test — observed on the HSA San Antonio. (c) Average annual percentage of diabetic Medicare enrollees age 65-75 having hemoglobin A1c test — predicted on the partitioning units of San Antonio.

and find that MS-MCAR appears to have higher prediction errors and are robust under model misspecification while is computationally at a disadvantage compared to MS-SRE and MS-OH.

We include a motivating data analysis which shows the benefits of our bivariate multiscale approaches. Specifically, we look at the blood test monitoring data in Texas from the Dartmouth Atlas Project. We fit the MS-SRE, MS-MCAR, and MS-OH to jointly model two different blood tests that can be used as a hospital quality measure. Each blood test considered has a different scale, as one of them is observed on Texas hospital service areas and the other is observed on Texas counties. Through visually examining the prediction plots on the partition scale and comparing the WAICs, we reach the conclusion that MS-MCAR performs the best in terms of prediction accuracy. Reasonable predictions can also be made from MS-SRE and MS-OH, which are computationally much more efficient than MS-MCAR as shown in the simulation.

Notice that in our illustrations the COS is performed by choosing a target support that is different from the two source supports. Based on that choice, our models allow for the COS for both variables. It is important to note that our models do not restrict the choice of target support to be the one we use. For example, we could choose to predict on one of the source supports, in which case COS is done for only one of the variables by the models. Our models allow for COS to any scale we are interested, which can be achieved through specifying a different partition matrix \mathbf{P} based on the partition of the source supports and target support chosen. The flexibility of our models allows them to be widely applied in other bivariate multiscale spatial settings.

There are still many avenues for future research. One possible extension of our work is to consider non-Gaussian data. Our work is based on the assumption that both responses follow a Gaussian distribution. However, this may not always be true as, for example, survey data that sometimes requires multiscale analysis tends to be Poisson distributed (Bradley et al., 2016; Mugglin & Carlin, 1998; Mugglin et al., 1999). Moreover, our models are presented in spatial-only and bivariate settings. Extension of our models to consider spatio-temporal or higher dimensional multivariate settings may be needed. The implementation of our models

depends heavily on the MCMC. The Metropolis-Hastings steps within the Gibbs sampler for updating certain parameters create difficulty as the tuning requires substantial amount of time and effort. Considering these computational difficulties when the sample size is large, more efficient methods should be considered.

Acknowledgments

This research was partially supported by the U.S. National Science Foundation (NSF) under NSF grant 2310756.

References

- Banerjee, S., Carlin, B.P. & Gelfand, A.E. (2015) *Hierarchical Modeling and Analysis for Spatial Data*. London, UK: Chapman and Hall.
- Banerjee, S., Gelfand, A.E., Finley, A.O. & Sang, H. (2008) Gaussian predictive process models for large spatial data sets. *Journal of the Royal Statistical Society: Series B*, 70(4), 825–848.
- Benedetti, M.H., Berrocal, V.J. & Little, R.J. (2022) Accounting for survey design in Bayesian disaggregation of survey-based areal estimates of proportions: An application to the American Community Survey. *Annals of Applied Statistics*, 16(4), 2201–2230.
- Bradley, J.R., Holan, S.H. & Wikle, C.K. (2015) Multivariate Spatio-Temporal Models for High-Dimensional Areal Data with Application to Longitudinal Employer-Household Dynamics. *The Annals of Applied Statistics*, 9(4), 1761–1791.
- Bradley, J.R., Holan, S.H. & Wikle, C.K. (2018) Computationally Efficient Multivariate Spatio-Temporal Models for High-Dimensional Count-Valued Data (with Discussion). *Bayesian Analysis*, 13(1), 253–310.
- Bradley, J.R., Wikle, C.K. & Holan, S.H. (2016) Bayesian Spatial Change of Support for Count-Valued Survey Data with Application to the American Community Survey. *Journal of the American Statistical Association*, 111(514), 472–487.
- Bradley, J.R., Wikle, C.K. & Holan, S.H. (2017) Regionalization of multiscale spatial processes by using a criterion for spatial aggregation error. *Journal of the Royal Statistical Society: Series B*, 79(3), 815–832.
- Carlin, B.P. & Banerjee, S. (2003) Hierarchical Multivariate CAR Models for Spatio-Temporally Correlated Survival Data. *Bayesian Statistics*, 7, 45–63.
- Cressie, N. & Johannesson G. (2008) Fixed Rank Kriging for Very Large Spatial Data Sets. *Journal of the Royal Statistical Society: Series B*, 70(1), 209–226.
- Dartmouth Atlas Data (2022) Selected Primary Care Access and Quality Measures. Available at <https://data.dartmouthatlas.org/primary-care/>.

- Daw, R., Simpson, M., Wikle, C.K., Holan, S.H. & Bradley, J.R. (2022) An Overview of Univariate and Multivariate Karhunen Loève Expansions in Statistics. *Journal of the Indian Society for Probability and Statistics*, 23, 285–326.
- Delamater, A.M. (2006) Clinical Use of Hemoglobin A1c to Improve Diabetes Management. *Clinical Diabetes*, 24(1), 6–8.
- Gelfand, A.E. & Vounatsou, P. (2003) Proper multivariate conditional autoregressive models for spatial data analysis. *Biostatistics*, 4(1), 11–25.
- Gelfand, A.E., Zhu, L. & Carlin B.P. (2001) On the change of support problem for spatio-temporal data. *Biostatistics*, 2(1), 31–45.
- Gelman, A. & Rubin D.B. (1992) Inference from Iterative Simulation Using Multiple Sequences. *Statistical Science*, 7(4), 457–472.
- Gotway, C.A. & Young L.J. (2002) Combining Incompatible Spatial Data. *Journal of the American Statistical Association*, 97(458), 632–648.
- Habib, S.S. & Aslam, M. (2003) Risk factors, knowledge and health status in diabetic patients. *Saudi Medical Journal*, 24(11), 1219–1224.
- Hughes, J. & Haran, M. (2013) Dimension reduction and alleviation of confounding for spatial generalized linear mixed models. *Journal of the Royal Statistical Society: Series B*, 75(1), 139–159.
- Khan, K. & Calder, C.A. (2022) Restricted Spatial Regression Methods: Implications for Inference. *Journal of the American Statistical Association*, 117(537), 482–494.
- Kirkman, M.S., Briscoe, V.J., Clark, N., Florez, H., Haas, L.B., Halter, J.B., Huang, E.S., Korytkowski, M.T., Munshi, M.N., Odegard, P.S., Pratley, R.E. & Swift, C.S. (2012) Diabetes in Older Adults. *Diabetes Care*, 35(12), 2650–2664.
- Larsen, M.L., Horder, M. & Mogensen E.F. (1990) Effect of Long-Term Monitoring of Glycosylated Hemoglobin Levels in Insulin-Dependent Diabetes Mellitus. *The New England Journal of Medicine*, 323(15), 1021–1025.
- Mardia, K.V. & Goodall C.R. (1993) Spatial-Temporal Analysis of Multivariate Environmental Monitoring Data. *Multivariate Environmental Statistics* (pp. 347–386). Elsevier Science Publishers B.V.
- Messick, R.M., Heaton, M.J. & Hansen, N. (2017) Multivariate spatial mapping of soil water holding capacity with spatially varying cross-correlations. *Annals of Applied Statistics*, 11(1), 69–92.
- Moran, P.A.P. (1950) Notes on Continuous Stochastic Phenomena. *Biometrika*, 37(1), 17–23.
- Mugglin, A.S. & Carlin, B.P. (1998) Hierarchical Modeling in Geographic Information Systems: Population Interpolation over Incompatible Zones. *Journal of Agricultural, Biological, and Environmental Statistics*, 3(2), 111–130.

- Mugglin, A.S., Carlin, B.P., Zhu, L. & Conlon, E. (1999) Bayesian Areal Interpolation, Estimation, and Smoothing: An Inferential Approach for Geographic Information Systems. *Environment and Planning A*, 31(8), 1337–1352.
- Obled, C. & Creutin, J. (1986) Some developments in the use of empirical orthogonal functions for mapping meteorological fields. *Journal of Applied Meteorology*, 25(9), 1189–1204.
- Qu, K., Bradley, J.R. & Niu, X. (2021) Boundary Detection Using a Bayesian Hierarchical Model for Multiscale Spatial Data. *Technometrics*, 63(1), 64–76.
- Raim, A.M., Holan, S.H., Bradley, J.R. & Wikle, C.K. (2021) Spatio-temporal change of support modeling with R. *Computational Statistics*, 36, 749–780.
- Royle, J.A. & Berliner, L.M. (1999) A Hierarchical Approach to Multivariate Spatial Modeling and Prediction. *Journal of Agricultural, Biological, and Environmental Statistics*, 4(1), 29–56.
- Waller, L.A. & Gotway, C.A. (2004) *Applied Spatial Statistics for Public Health Data*. Hoboken, NJ: Wiley.
- Watanabe, S. (2010) Asymptotic Equivalence of Bayes Cross Validation and Widely Applicable Information Criterion in Singular Learning Theory. *The Journal of Machine Learning Research*, 11, 3571–3594.
- Wikle, C.K. & Berliner L.M. (2005) Combining Information across Spatial Scales. *Technometrics*, 47(1), 80–91.

Appendix A Full Conditional Distributions

In this appendix, we provide the derivation of full conditional distributions for all three models, namely, MS-SRE, MS-MCAR, and MS-OH.

A.1 Derivation of full conditional distributions for MS-SRE

Consider the MS-SRE model specified in Table 2, the full conditional distribution for $\boldsymbol{\eta}$ can be written as,

$$\begin{aligned}
f(\boldsymbol{\eta}|\cdot) &\propto \prod_{i=1}^{n_1} f(Y_1(B_i)|\beta_1, \boldsymbol{\eta}, \sigma_1^2) \cdot \prod_{j=1}^{n_2} f(Y_2(C_j)|\beta_2, \boldsymbol{\eta}, \sigma_2^2) \cdot f(\boldsymbol{\eta}|\sigma_\eta^2, \phi) \\
&\propto \exp \left(\sum_{i=1}^{n_1} -\frac{1}{2\sigma_1^2(\mathbf{P}_1\mathbf{P}'_1)_{ii}} (Y_1(B_i) - \beta_1 - \mathbf{g}_1(B_i)'\boldsymbol{\eta})^2 \right. \\
&\quad \left. - \sum_{j=1}^{n_2} \frac{1}{2\sigma_2^2(\mathbf{P}_2\mathbf{P}'_2)_{jj}} (Y_2(C_j) - \beta_2 - \mathbf{g}_2(C_j)'\boldsymbol{\eta})^2 - \frac{1}{2}\boldsymbol{\eta}'\mathbf{K}^{-1}\boldsymbol{\eta} \right) \\
&\propto \exp \left(\sum_{i=1}^{n_1} -\frac{1}{2\sigma_1^2(\mathbf{P}_1\mathbf{P}'_1)_{ii}} \boldsymbol{\eta}'\mathbf{g}_1(B_i)\mathbf{g}_1(B_i)'\boldsymbol{\eta} + \sum_{i=1}^{n_1} \frac{1}{\sigma_1^2(\mathbf{P}_1\mathbf{P}'_1)_{ii}} \mathbf{g}_1(B_i)'\boldsymbol{\eta}(Y_1(B_i) - \beta_1) \right. \\
&\quad \left. - \sum_{j=1}^{n_2} \frac{1}{2\sigma_2^2(\mathbf{P}_2\mathbf{P}'_2)_{jj}} \boldsymbol{\eta}'\mathbf{g}_2(C_j)\mathbf{g}_2(C_j)'\boldsymbol{\eta} + \sum_{j=1}^{n_2} \frac{1}{\sigma_2^2(\mathbf{P}_2\mathbf{P}'_2)_{jj}} \mathbf{g}_2(C_j)'\boldsymbol{\eta}(Y_2(C_j) - \beta_2) - \frac{1}{2}\boldsymbol{\eta}'\mathbf{K}^{-1}\boldsymbol{\eta} \right) \\
&= \exp \left\{ -\frac{1}{2} \left[\boldsymbol{\eta}' \left(\sum_{i=1}^{n_1} \frac{\mathbf{g}_1(B_i)\mathbf{g}_1(B_i)'}{\sigma_1^2(\mathbf{P}_1\mathbf{P}'_1)_{ii}} + \sum_{j=1}^{n_2} \frac{\mathbf{g}_2(C_j)\mathbf{g}_2(C_j)'}{\sigma_2^2(\mathbf{P}_2\mathbf{P}'_2)_{jj}} + \mathbf{K}^{-1} \right) \boldsymbol{\eta} \right. \right. \\
&\quad \left. \left. - 2 \left(\sum_{i=1}^{n_1} \frac{\mathbf{g}_1(B_i)'\mathbf{g}_1(B_i)(Y_1(B_i) - \beta_1)}{\sigma_1^2(\mathbf{P}_1\mathbf{P}'_1)_{ii}} + \sum_{j=1}^{n_2} \frac{\mathbf{g}_2(C_j)'\mathbf{g}_2(C_j)(Y_2(C_j) - \beta_2)}{\sigma_2^2(\mathbf{P}_2\mathbf{P}'_2)_{jj}} \right) \boldsymbol{\eta} \right] \right\} \\
&= \exp \left(-\frac{1}{2}(\boldsymbol{\eta}'\mathbf{B}^{-1}\boldsymbol{\eta} - 2\mathbf{b}'\boldsymbol{\eta}) \right) \\
&\propto \exp \left(-\frac{1}{2}(\boldsymbol{\eta}'\mathbf{B}^{-1}\boldsymbol{\eta} - 2\mathbf{b}'\mathbf{B}\mathbf{B}^{-1}\boldsymbol{\eta} + \mathbf{b}'\mathbf{B}\mathbf{b}) \right) \\
&= \exp \left(-\frac{1}{2}(\boldsymbol{\eta} - \mathbf{B}\mathbf{b})'\mathbf{B}^{-1}(\boldsymbol{\eta} - \mathbf{B}\mathbf{b}) \right) \\
&\propto MVN(\mathbf{B}\mathbf{b}, \mathbf{B})
\end{aligned}$$

where $\mathbf{B}^{-1} = \sum_{i=1}^{n_1} \frac{\mathbf{g}_1(B_i)\mathbf{g}_1(B_i)'}{\sigma_1^2(\mathbf{P}_1\mathbf{P}'_1)_{ii}} + \sum_{j=1}^{n_2} \frac{\mathbf{g}_2(C_j)\mathbf{g}_2(C_j)'}{\sigma_2^2(\mathbf{P}_2\mathbf{P}'_2)_{jj}} + \mathbf{K}^{-1}$ and $\mathbf{b}' = \sum_{i=1}^{n_1} \frac{\mathbf{g}_1(B_i)'\mathbf{g}_1(B_i)(Y_1(B_i) - \beta_1)}{\sigma_1^2(\mathbf{P}_1\mathbf{P}'_1)_{ii}} + \sum_{j=1}^{n_2} \frac{\mathbf{g}_2(C_j)'\mathbf{g}_2(C_j)(Y_2(C_j) - \beta_2)}{\sigma_2^2(\mathbf{P}_2\mathbf{P}'_2)_{jj}}$. Similarly, the full conditional distributions for $\beta_1, \beta_2, \sigma_\eta^2, \sigma_1^2, \sigma_2^2$, and ϕ can be derived as follows,

$$f(\beta_1|\cdot) \propto \prod_{i=1}^{n_1} f(Y_1(B_i)|\beta_1, \boldsymbol{\eta}, \sigma_1^2) \cdot f(\beta_1)$$

$$\begin{aligned}
& \propto \exp \left(\sum_{i=1}^{n_1} -\frac{1}{2\sigma_1^2(\mathbf{P}_1\mathbf{P}'_1)_{ii}} (Y_1(B_i) - \beta_1 - \mathbf{g}_1(B_i)'\boldsymbol{\eta})^2 - \frac{1}{2\sigma_\beta^2}\beta_1^2 \right) \\
& \propto \exp \left[\beta_1^2 \left(-\sum_{i=1}^{n_1} \frac{1}{2\sigma_1^2(\mathbf{P}_1\mathbf{P}'_1)_{ii}} - \frac{1}{2\sigma_\beta^2} \right) - \beta_1 \left(-\sum_{i=1}^{n_1} \frac{Y_1(B_i) - \mathbf{g}_1(B_i)'\boldsymbol{\eta}}{\sigma_1^2(\mathbf{P}_1\mathbf{P}'_1)_{ii}} \right) \right] \\
& = \exp(a\beta_1^2 - b\beta_1) \\
& = \exp \left(\frac{\beta_1^2 - \frac{b}{a}\beta_1}{1/a} \right) \\
& = \exp \left(\frac{\beta_1^2 - 2\frac{b}{2a}\beta_1 + (\frac{b}{2a})^2 - (\frac{b}{2a})^2}{1/a} \right) \\
& \propto \exp \left(\frac{(\beta_1 - \frac{b}{2a})^2}{1/a} \right) \\
& = \exp \left(\frac{(\beta_1 - \frac{b}{2a})^2}{-2(-\frac{1}{2a})} \right) \\
& \propto N \left(\frac{b}{2a}, -\frac{1}{2a} \right) \quad \text{where } a = -\sum_{i=1}^{n_1} \frac{1}{2\sigma_1^2(\mathbf{P}_1\mathbf{P}'_1)_{ii}} - \frac{1}{2\sigma_\beta^2} \text{ and } b = -\sum_{i=1}^{n_1} \frac{Y_1(B_i) - \mathbf{g}_1(B_i)'\boldsymbol{\eta}}{\sigma_1^2(\mathbf{P}_1\mathbf{P}'_1)_{ii}}
\end{aligned}$$

$$f(\beta_2|\cdot) \propto \prod_{j=1}^{n_2} f(Y_2(C_j)|\beta_2, \boldsymbol{\eta}, \sigma_2^2) \cdot f(\beta_2)$$

$$\begin{aligned}
& \propto \exp \left(\sum_{j=1}^{n_2} -\frac{1}{2\sigma_2^2(\mathbf{P}_2\mathbf{P}'_2)_{jj}} (Y_2(C_j) - \beta_2 - \mathbf{g}_2(C_j)'\boldsymbol{\eta})^2 - \frac{1}{2\sigma_\beta^2}\beta_2^2 \right) \\
& \propto \exp \left[\beta_2^2 \left(-\sum_{j=1}^{n_2} \frac{1}{2\sigma_2^2(\mathbf{P}_2\mathbf{P}'_2)_{jj}} - \frac{1}{2\sigma_\beta^2} \right) - \beta_2 \left(-\sum_{j=1}^{n_2} \frac{Y_2(C_j) - \mathbf{g}_2(C_j)'\boldsymbol{\eta}}{\sigma_2^2(\mathbf{P}_2\mathbf{P}'_2)_{jj}} \right) \right] \\
& = \exp(a\beta_2^2 - b\beta_2) \\
& = \exp \left(\frac{\beta_2^2 - \frac{b}{a}\beta_2}{1/a} \right) \\
& = \exp \left(\frac{\beta_2^2 - 2\frac{b}{2a}\beta_2 + (\frac{b}{2a})^2 - (\frac{b}{2a})^2}{1/a} \right) \\
& \propto \exp \left(\frac{(\beta_2 - \frac{b}{2a})^2}{1/a} \right) \\
& = \exp \left(\frac{(\beta_2 - \frac{b}{2a})^2}{-2(-\frac{1}{2a})} \right) \\
& \propto N \left(\frac{b}{2a}, -\frac{1}{2a} \right) \quad \text{where } a = -\sum_{j=1}^{n_2} \frac{1}{2\sigma_2^2(\mathbf{P}_2\mathbf{P}'_2)_{jj}} - \frac{1}{2\sigma_\beta^2} \text{ and } b = -\sum_{j=1}^{n_2} \frac{Y_2(C_j) - \mathbf{g}_2(C_j)'\boldsymbol{\eta}}{\sigma_2^2(\mathbf{P}_2\mathbf{P}'_2)_{jj}}
\end{aligned}$$

$$f(\sigma_\eta^2|\cdot) \propto f(\boldsymbol{\eta}|\sigma_\eta^2, \phi) \cdot f(\sigma_\eta^2)$$

$$\begin{aligned}
& \propto (\sigma_\eta^2)^{-a_\eta-1} \exp\left(-\frac{b_\eta}{\sigma_\eta^2}\right) \cdot |\{\sigma_\eta^2 \exp(-\phi \|\mathbf{c}_i - \mathbf{c}_j\|)\}|^{-1/2} \exp\left(-\frac{1}{2} \boldsymbol{\eta}' \{\sigma_\eta^2 \exp(-\phi \|\mathbf{c}_i - \mathbf{c}_j\|)\}^{-1} \boldsymbol{\eta}\right) \\
& \propto (\sigma_\eta^2)^{-a_\eta-1} \exp\left(-\frac{b_\eta}{\sigma_\eta^2}\right) (\sigma_\eta^2)^{-r/2} \exp\left(-\frac{1}{2\sigma_\eta^2} \boldsymbol{\eta}' \{\exp(-\phi \|\mathbf{c}_i - \mathbf{c}_j\|)\}^{-1} \boldsymbol{\eta}\right) \\
& = (\sigma_\eta^2)^{-(a_\eta + \frac{r}{2})-1} \exp\left(-\frac{b_\eta + \frac{1}{2} \boldsymbol{\eta}' \{\exp(-\phi \|\mathbf{c}_i - \mathbf{c}_j\|)\}^{-1} \boldsymbol{\eta}}{\sigma_\eta^2}\right) \\
& \propto IG\left(a_\eta + \frac{r}{2}, b_\eta + \frac{1}{2} \boldsymbol{\eta}' \{\exp(-\phi \|\mathbf{c}_i - \mathbf{c}_j\|)\}^{-1} \boldsymbol{\eta}\right) \\
f(\sigma_1^2 | \cdot) & \propto \prod_{i=1}^{n_1} f(Y_1(B_i) | \beta_1, \boldsymbol{\eta}, \sigma_1^2) \cdot f(\sigma_1^2) \\
& \propto \prod_{i=1}^{n_1} \left(\frac{1}{\sqrt{2\pi\sigma_1^2(\mathbf{P}_1\mathbf{P}'_1)_{ii}}} \exp\left(-\frac{1}{2\sigma_1^2(\mathbf{P}_1\mathbf{P}'_1)_{ii}} (Y_1(B_i) - \beta_1 - \mathbf{g}_1(B_i)' \boldsymbol{\eta})^2\right) \right) \\
& \quad \cdot (\sigma_1^2)^{-a_\sigma-1} \exp\left(-\frac{b_\sigma}{\sigma_1^2}\right) \\
& \propto (\sigma_1^2)^{-(a_\sigma + \frac{n_1}{2})-1} \exp\left(-\frac{b_\sigma + \sum_{i=1}^{n_1} \frac{1}{2(\mathbf{P}_1\mathbf{P}'_1)_{ii}} (Y_1(B_i) - \beta_1 - \mathbf{g}_1(B_i)' \boldsymbol{\eta})^2}{\sigma_1^2}\right) \\
& \propto IG\left(a_\sigma + \frac{n_1}{2}, b_\sigma + \sum_{i=1}^{n_1} \frac{1}{2(\mathbf{P}_1\mathbf{P}'_1)_{ii}} (Y_1(B_i) - \beta_1 - \mathbf{g}_1(B_i)' \boldsymbol{\eta})^2\right) \\
f(\sigma_2^2 | \cdot) & \propto \prod_{j=1}^{n_2} f(Y_2(C_j) | \beta_2, \boldsymbol{\eta}, \sigma_2^2) \cdot f(\sigma_2^2) \\
& \propto \prod_{j=1}^{n_2} \left(\frac{1}{\sqrt{2\pi\sigma_2^2(\mathbf{P}_2\mathbf{P}'_2)_{jj}}} \exp\left(-\frac{1}{2\sigma_2^2(\mathbf{P}_2\mathbf{P}'_2)_{jj}} (Y_2(C_j) - \beta_2 - \mathbf{g}_2(C_j)' \boldsymbol{\eta})^2\right) \right) \\
& \quad \cdot (\sigma_2^2)^{-a_\sigma-1} \exp\left(-\frac{b_\sigma}{\sigma_2^2}\right) \\
& \propto (\sigma_2^2)^{-(a_\sigma + \frac{n_2}{2})-1} \exp\left(-\frac{b_\sigma + \sum_{j=1}^{n_2} \frac{1}{2(\mathbf{P}_2\mathbf{P}'_2)_{jj}} (Y_2(C_j) - \beta_2 - \mathbf{g}_2(C_j)' \boldsymbol{\eta})^2}{\sigma_2^2}\right) \\
& \propto IG\left(a_\sigma + \frac{n_2}{2}, b_\sigma + \sum_{j=1}^{n_2} \frac{1}{2(\mathbf{P}_2\mathbf{P}'_2)_{jj}} (Y_2(C_j) - \beta_2 - \mathbf{g}_2(C_j)' \boldsymbol{\eta})^2\right) \\
f(\phi | \cdot) & \propto f(\boldsymbol{\eta} | \sigma_\eta^2, \phi) \cdot f(\phi) \\
& \propto |\{\sigma_\eta^2 \exp(-\phi \|\mathbf{c}_i - \mathbf{c}_j\|)\}|^{-1/2} \exp\left(-\frac{1}{2} \boldsymbol{\eta}' \{\sigma_\eta^2 \exp(-\phi \|\mathbf{c}_i - \mathbf{c}_j\|)\}^{-1} \boldsymbol{\eta}\right) \cdot \frac{1}{b_\phi - a_\phi}
\end{aligned}$$

Note that the full conditional distribution for ϕ does not have a closed form. Therefore, the update of ϕ requires a Metropolis-Hastings step within the Gibbs sampler.

A.2 Derivation of full conditional distributions for MS-MCAR

We first derive the full conditional distribution for $\boldsymbol{\psi}$ in the MS-MCAR model specified in Table 2,

$$\begin{aligned}
f(\boldsymbol{\psi}|\cdot) &\propto \prod_{i=1}^{n_1} f(Y_1(B_i)|\beta_1, \boldsymbol{\psi}, \sigma_1^2) \cdot \prod_{j=1}^{n_2} f(Y_2(C_j)|\beta_2, \boldsymbol{\psi}, \sigma_2^2) \cdot f(\boldsymbol{\psi}|\rho, \tau, \nu^2) \\
&\propto \exp \left(\sum_{i=1}^{n_1} -\frac{1}{2\sigma_1^2(\mathbf{P}_1\mathbf{P}'_1)_{ii}} (Y_1(B_i) - \beta_1 - \mathbf{p}(B_i)'\boldsymbol{\psi})^2 \right. \\
&\quad \left. - \sum_{j=1}^{n_2} \frac{1}{2\sigma_2^2(\mathbf{P}_2\mathbf{P}'_2)_{jj}} (Y_2(C_j) - \beta_2 - \mathbf{p}(C_j)'\boldsymbol{\psi})^2 - \frac{1}{2}\boldsymbol{\psi}'(\boldsymbol{\Sigma} \otimes (\mathbf{D} - \rho\mathbf{W})^{-1})^{-1}\boldsymbol{\psi} \right) \\
&\propto \exp \left(-\frac{1}{2} \left[\boldsymbol{\psi}' \left(\sum_{i=1}^{n_1} \frac{\mathbf{p}(B_i)\mathbf{p}(B_i)'}{\sigma_1^2(\mathbf{P}_1\mathbf{P}'_1)_{ii}} + \sum_{j=1}^{n_2} \frac{\mathbf{p}(C_j)\mathbf{p}(C_j)'}{\sigma_2^2(\mathbf{P}_2\mathbf{P}'_2)_{jj}} + (\boldsymbol{\Sigma} \otimes (\mathbf{D} - \rho\mathbf{W})^{-1})^{-1} \right) \boldsymbol{\psi} \right. \right. \\
&\quad \left. \left. - 2 \left(\sum_{i=1}^{n_1} \frac{\mathbf{p}(B_i)'(Y_1(B_i) - \beta_1)}{\sigma_1^2(\mathbf{P}_1\mathbf{P}'_1)_{ii}} + \sum_{j=1}^{n_2} \frac{\mathbf{p}(C_j)'(Y_2(C_j) - \beta_2)}{\sigma_2^2(\mathbf{P}_2\mathbf{P}'_2)_{jj}} \right) \boldsymbol{\psi} \right] \right) \\
&= \exp \left(-\frac{1}{2}(\boldsymbol{\psi}'\mathbf{B}^{-1}\boldsymbol{\psi} - 2\mathbf{b}'\boldsymbol{\psi}) \right) \\
&\propto \exp \left(-\frac{1}{2}(\boldsymbol{\psi}'\mathbf{B}^{-1}\boldsymbol{\psi} - 2\mathbf{b}'\mathbf{B}\mathbf{B}^{-1}\boldsymbol{\psi} + \mathbf{b}'\mathbf{B}\mathbf{b}) \right) \\
&= \exp \left(-\frac{1}{2}(\boldsymbol{\psi} - \mathbf{B}\mathbf{b})'\mathbf{B}^{-1}(\boldsymbol{\psi} - \mathbf{B}\mathbf{b}) \right) \\
&\propto MVN(\mathbf{B}\mathbf{b}, \mathbf{B})
\end{aligned}$$

where $\mathbf{B}^{-1} = \sum_{i=1}^{n_1} \frac{\mathbf{p}(B_i)\mathbf{p}(B_i)'}{\sigma_1^2(\mathbf{P}_1\mathbf{P}'_1)_{ii}} + \sum_{j=1}^{n_2} \frac{\mathbf{p}(C_j)\mathbf{p}(C_j)'}{\sigma_2^2(\mathbf{P}_2\mathbf{P}'_2)_{jj}} + (\boldsymbol{\Sigma} \otimes (\mathbf{D} - \rho\mathbf{W})^{-1})^{-1}$ and $\mathbf{b}' = \sum_{i=1}^{n_1} \frac{\mathbf{p}(B_i)'(Y_1(B_i) - \beta_1)}{\sigma_1^2(\mathbf{P}_1\mathbf{P}'_1)_{ii}} + \sum_{j=1}^{n_2} \frac{\mathbf{p}(C_j)'(Y_2(C_j) - \beta_2)}{\sigma_2^2(\mathbf{P}_2\mathbf{P}'_2)_{jj}}$. The full conditional distributions for $\beta_1, \beta_2, \rho, \tau, \nu^2, \sigma_1^2$ and σ_2^2 can be derived similarly as follows,

$$\begin{aligned}
f(\beta_1|\cdot) &\propto \prod_{i=1}^{n_1} f(Y_1(B_i)|\beta_1, \boldsymbol{\psi}, \sigma_1^2) \cdot f(\beta_1) \\
&\propto \exp \left(-\sum_{i=1}^{n_1} \frac{1}{2\sigma_1^2(\mathbf{P}_1\mathbf{P}'_1)_{ii}} (Y_1(B_i) - \beta_1 - \mathbf{p}(B_i)'\boldsymbol{\psi})^2 - \frac{1}{2\sigma_\beta^2}\beta_1^2 \right) \\
&\propto \exp \left(\beta_1^2 \left(-\sum_{i=1}^{n_1} \frac{1}{2\sigma_1^2(\mathbf{P}_1\mathbf{P}'_1)_{ii}} - \frac{1}{2\sigma_\beta^2} \right) - \beta_1 \left(-\sum_{i=1}^{n_1} \frac{Y_1(B_i) - \mathbf{p}(B_i)'\boldsymbol{\psi}}{\sigma_1^2(\mathbf{P}_1\mathbf{P}'_1)_{ii}} \right) \right) \\
&= \exp(a\beta_1^2 - b\beta_1) \\
&= \exp \left(\frac{\beta_1^2 - \frac{b}{a}\beta_1}{1/a} \right)
\end{aligned}$$

$$\begin{aligned}
&= \exp\left(\frac{\beta_1^2 - 2\frac{b}{2a}\beta_1 + (\frac{b}{2a})^2 - (\frac{b}{2a})^2}{1/a}\right) \\
&\propto \exp\left(\frac{(\beta_1 - \frac{b}{2a})^2}{1/a}\right) \\
&= \exp\left(\frac{(\beta_1 - \frac{b}{2a})^2}{-2(-\frac{1}{2a})}\right) \\
&\propto N\left(\frac{b}{2a}, -\frac{1}{2a}\right) \quad \text{where } a = -\sum_{i=1}^{n_1} \frac{1}{2\sigma_1^2(\mathbf{P}_1\mathbf{P}'_1)_{ii}} - \frac{1}{2\sigma_\beta^2} \text{ and } b = -\sum_{i=1}^{n_1} \frac{Y_1(B_i) - \mathbf{p}(B_i)'\boldsymbol{\psi}}{\sigma_1^2(\mathbf{P}_1\mathbf{P}'_1)_{ii}} \\
f(\beta_2|\cdot) &\propto \prod_{j=1}^{n_2} f(Y_2(C_j)|\beta_2, \boldsymbol{\psi}, \sigma_2^2) \cdot f(\beta_2) \\
&\propto \exp\left(-\sum_{j=1}^{n_2} \frac{1}{2\sigma_2^2(\mathbf{P}_2\mathbf{P}'_2)_{jj}} (Y_2(C_j) - \beta_2 - \mathbf{p}(C_j)'\boldsymbol{\psi})^2 - \frac{1}{2\sigma_\beta^2}\beta_2^2\right) \\
&\propto \exp\left(\beta_2^2\left(-\sum_{j=1}^{n_2} \frac{1}{2\sigma_2^2(\mathbf{P}_2\mathbf{P}'_2)_{jj}} - \frac{1}{2\sigma_\beta^2}\right) - \beta_2\left(-\sum_{j=1}^{n_2} \frac{Y_2(C_j) - \mathbf{p}(C_j)'\boldsymbol{\psi}}{\sigma_2^2(\mathbf{P}_2\mathbf{P}'_2)_{jj}}\right)\right) \\
&= \exp(a\beta_2^2 - b\beta_2) \\
&= \exp\left(\frac{\beta_2^2 - \frac{b}{a}\beta_2}{1/a}\right) \\
&= \exp\left(\frac{\beta_2^2 - 2\frac{b}{2a}\beta_2 + (\frac{b}{2a})^2 - (\frac{b}{2a})^2}{1/a}\right) \\
&\propto \exp\left(\frac{(\beta_2 - \frac{b}{2a})^2}{1/a}\right) \\
&= \exp\left(\frac{(\beta_2 - \frac{b}{2a})^2}{-2(-\frac{1}{2a})}\right) \\
&\propto N\left(\frac{b}{2a}, -\frac{1}{2a}\right) \quad \text{where } a = -\sum_{j=1}^{n_2} \frac{1}{2\sigma_2^2(\mathbf{P}_2\mathbf{P}'_2)_{jj}} - \frac{1}{2\sigma_\beta^2} \text{ and } b = -\sum_{j=1}^{n_2} \frac{Y_2(C_j) - \mathbf{p}(C_j)'\boldsymbol{\psi}}{\sigma_2^2(\mathbf{P}_2\mathbf{P}'_2)_{jj}} \\
f(\rho|\cdot) &\propto f(\boldsymbol{\psi}|\rho, \tau, \nu^2) \cdot f(\rho) \\
&\propto |\boldsymbol{\Sigma} \otimes (\mathbf{D} - \rho\mathbf{W})^{-1}|^{-1/2} \exp\left(-\frac{1}{2}\boldsymbol{\psi}'[\boldsymbol{\Sigma} \otimes (\mathbf{D} - \rho\mathbf{W})^{-1}]^{-1}\boldsymbol{\psi}\right) \cdot \frac{1}{b_\rho - a_\rho} \\
f(\tau|\cdot) &\propto f(\boldsymbol{\psi}|\rho, \tau, \nu^2) \cdot f(\tau) \\
&\propto |\boldsymbol{\Sigma} \otimes (\mathbf{D} - \rho\mathbf{W})^{-1}|^{-1/2} \exp\left(-\frac{1}{2}\boldsymbol{\psi}'[\boldsymbol{\Sigma} \otimes (\mathbf{D} - \rho\mathbf{W})^{-1}]^{-1}\boldsymbol{\psi}\right) \cdot \frac{1}{b_\tau - a_\tau} \\
f(\nu^2|\cdot) &\propto f(\boldsymbol{\psi}|\rho, \tau, \nu^2) \cdot f(\nu^2) \\
&\propto |\boldsymbol{\Sigma} \otimes (\mathbf{D} - \rho\mathbf{W})^{-1}|^{-1/2} \exp\left(-\frac{1}{2}\boldsymbol{\psi}'[\boldsymbol{\Sigma} \otimes (\mathbf{D} - \rho\mathbf{W})^{-1}]^{-1}\boldsymbol{\psi}\right) \cdot (\nu^2)^{-a_\nu-1} \exp\left(-\frac{b_\nu}{\nu^2}\right)
\end{aligned}$$

$$\begin{aligned}
& \propto (\nu^2)^{-2n_3/2} \exp\left(-\frac{1}{2\nu^2} \boldsymbol{\psi}' [\mathbf{T}(\tau)^{-1} \otimes (\mathbf{D} - \rho \mathbf{W})] \boldsymbol{\psi}\right) \cdot (\nu^2)^{-a_\nu-1} \exp\left(-\frac{b_\nu}{\nu^2}\right) \\
& \propto (\nu^2)^{-n_3-a_\nu-1} \exp\left(-\frac{b_\nu + \frac{1}{2} \boldsymbol{\psi}' [\mathbf{T}(\tau)^{-1} \otimes (\mathbf{D} - \rho \mathbf{W})] \boldsymbol{\psi}}{\nu^2}\right) \\
& \propto IG\left(a_\nu + n_3, b_\nu + \frac{1}{2} \boldsymbol{\psi}' [\mathbf{T}(\tau)^{-1} \otimes (\mathbf{D} - \rho \mathbf{W})] \boldsymbol{\psi}\right) \\
f(\sigma_1^2 | \cdot) & \propto \prod_{i=1}^{n_1} f(Y_1(B_i) | \beta_1, \boldsymbol{\psi}, \sigma_1^2) \cdot f(\sigma_1^2) \\
& \propto \prod_{i=1}^{n_1} \left(\frac{1}{\sqrt{2\pi\sigma_1^2(\mathbf{P}_1\mathbf{P}'_1)_{ii}}} \exp\left(-\frac{1}{2\sigma_1^2(\mathbf{P}_1\mathbf{P}'_1)_{ii}} (Y_1(B_i) - \beta_1 - \mathbf{p}(B_i)' \boldsymbol{\psi})^2\right) \right) \\
& \quad \cdot (\sigma_1^2)^{-a_\sigma-1} \exp\left(-\frac{b_\sigma}{\sigma_1^2}\right) \\
& \propto (\sigma_1^2)^{-(a_\sigma + \frac{n_1}{2})-1} \exp\left(-\frac{b_\sigma + \sum_{i=1}^{n_1} \frac{1}{2(\mathbf{P}_1\mathbf{P}'_1)_{ii}} (Y_1(B_i) - \beta_1 - \mathbf{p}(B_i)' \boldsymbol{\psi})^2}{\sigma_1^2}\right) \\
& \propto IG\left(a_\sigma + \frac{n_1}{2}, b_\sigma + \sum_{i=1}^{n_1} \frac{1}{2(\mathbf{P}_1\mathbf{P}'_1)_{ii}} (Y_1(B_i) - \beta_1 - \mathbf{p}(B_i)' \boldsymbol{\psi})^2\right) \\
f(\sigma_2^2 | \cdot) & \propto \prod_{j=1}^{n_2} f(Y_2(C_j) | \beta_2, \boldsymbol{\psi}, \sigma_2^2) \cdot f(\sigma_2^2) \\
& \propto \prod_{j=1}^{n_2} \left(\frac{1}{\sqrt{2\pi\sigma_2^2(\mathbf{P}_2\mathbf{P}'_2)_{jj}}} \exp\left(-\frac{1}{2\sigma_2^2(\mathbf{P}_2\mathbf{P}'_2)_{jj}} (Y_2(C_j) - \beta_2 - \mathbf{p}(C_j)' \boldsymbol{\psi})^2\right) \right) \\
& \quad \cdot (\sigma_2^2)^{-a_\sigma-1} \exp\left(-\frac{b_\sigma}{\sigma_2^2}\right) \\
& \propto (\sigma_2^2)^{-(a_\sigma + \frac{n_2}{2})-1} \exp\left(-\frac{b_\sigma + \sum_{j=1}^{n_2} \frac{1}{2(\mathbf{P}_2\mathbf{P}'_2)_{jj}} (Y_2(C_j) - \beta_2 - \mathbf{p}(C_j)' \boldsymbol{\psi})^2}{\sigma_2^2}\right) \\
& \propto IG\left(a_\sigma + \frac{n_2}{2}, b_\sigma + \sum_{j=1}^{n_2} \frac{1}{2(\mathbf{P}_2\mathbf{P}'_2)_{jj}} (Y_2(C_j) - \beta_2 - \mathbf{p}(C_j)' \boldsymbol{\psi})^2\right)
\end{aligned}$$

Note that the full conditional distributions for ρ and τ do not have closed forms. Therefore, Metropolis-Hastings steps are required for updating ρ and τ .

A.3 Derivation of full conditional distributions for MS-OH

Given the MS-OH model specified in Table 2, we can derive the full conditional distributions for $\boldsymbol{\eta}$, β_1 , β_2 , β_0 , σ_η^2 , σ_1^2 , σ_2^2 , and ϕ as follows,

$$f(\boldsymbol{\eta} | \cdot) \propto \prod_{i=1}^{n_1} f(Y_1(B_i) | \beta_1, \boldsymbol{\eta}, \sigma_1^2) \cdot \prod_{j=1}^{n_2} f(Y_2(C_j) | \beta_0, \beta_1, \beta_2, \boldsymbol{\eta}, \sigma_2^2) \cdot f(\boldsymbol{\eta} | \sigma_\eta^2, \phi)$$

$$\begin{aligned}
& \propto \exp \left(\sum_{i=1}^{n_1} -\frac{1}{2\sigma_1^2(\mathbf{P}_1\mathbf{P}'_1)_{ii}} (Y_1(B_i) - \beta_1 - \mathbf{g}_1(B_i)' \boldsymbol{\eta})^2 \right. \\
& \quad \left. - \sum_{j=1}^{n_2} \frac{1}{2\sigma_2^2(\mathbf{P}_2\mathbf{P}'_2)_{jj}} (Y_2(C_j) - \beta_0 - \beta_1\beta_2 - \beta_2\mathbf{g}_1(C_j)' \boldsymbol{\eta})^2 - \frac{1}{2} \boldsymbol{\eta}' \mathbf{K}^{-1} \boldsymbol{\eta} \right) \\
& \propto \exp \left(\sum_{i=1}^{n_1} -\frac{1}{2\sigma_1^2(\mathbf{P}_1\mathbf{P}'_1)_{ii}} [\boldsymbol{\eta}' \mathbf{g}_1(B_i) \mathbf{g}_1(B_i)' \boldsymbol{\eta} - 2\mathbf{g}_1(B_i)' \boldsymbol{\eta} (Y_1(B_i) - \beta_1)] \right. \\
& \quad \left. - \sum_{j=1}^{n_2} \frac{1}{2\sigma_2^2(\mathbf{P}_2\mathbf{P}'_2)_{jj}} [\beta_2^2 \boldsymbol{\eta}' \mathbf{g}_1(C_j) \mathbf{g}_1(C_j)' \boldsymbol{\eta} - 2\beta_2 \mathbf{g}_1(C_j)' \boldsymbol{\eta} (Y_2(C_j) - \beta_0 - \beta_1\beta_2)] - \frac{1}{2} \boldsymbol{\eta}' \mathbf{K}^{-1} \boldsymbol{\eta} \right) \\
& = \exp \left\{ -\frac{1}{2} \left[\boldsymbol{\eta}' \left(\sum_{i=1}^{n_1} \frac{\mathbf{g}_1(B_i) \mathbf{g}_1(B_i)'}{\sigma_1^2(\mathbf{P}_1\mathbf{P}'_1)_{ii}} + \sum_{j=1}^{n_2} \frac{\beta_2^2 \mathbf{g}_1(C_j) \mathbf{g}_1(C_j)'}{\sigma_2^2(\mathbf{P}_2\mathbf{P}'_2)_{jj}} + \mathbf{K}^{-1} \right) \boldsymbol{\eta} \right. \right. \\
& \quad \left. \left. - 2 \left(\sum_{i=1}^{n_1} \frac{\mathbf{g}_1(B_i)' (Y_1(B_i) - \beta_1)}{\sigma_1^2(\mathbf{P}_1\mathbf{P}'_1)_{ii}} + \sum_{j=1}^{n_2} \frac{\beta_2 \mathbf{g}_1(C_j)' (Y_2(C_j) - \beta_0 - \beta_1\beta_2)}{\sigma_2^2(\mathbf{P}_2\mathbf{P}'_2)_{jj}} \right) \boldsymbol{\eta} \right] \right\} \\
& = \exp \left(-\frac{1}{2} (\boldsymbol{\eta}' \mathbf{B}^{-1} \boldsymbol{\eta} - 2\mathbf{b}' \boldsymbol{\eta}) \right) \\
& \propto \exp \left(-\frac{1}{2} (\boldsymbol{\eta}' \mathbf{B}^{-1} \boldsymbol{\eta} - 2\mathbf{b}' \mathbf{B} \mathbf{B}^{-1} \boldsymbol{\eta} + \mathbf{b}' \mathbf{B} \mathbf{b}) \right) \\
& = \exp \left(-\frac{1}{2} (\boldsymbol{\eta} - \mathbf{B} \mathbf{b})' \mathbf{B}^{-1} (\boldsymbol{\eta} - \mathbf{B} \mathbf{b}) \right) \\
& \propto MVN(\mathbf{B} \mathbf{b}, \mathbf{B}) \quad \text{where } \mathbf{B}^{-1} = \sum_{i=1}^{n_1} \frac{\mathbf{g}_1(B_i) \mathbf{g}_1(B_i)'}{\sigma_1^2(\mathbf{P}_1\mathbf{P}'_1)_{ii}} + \sum_{j=1}^{n_2} \frac{\beta_2^2 \mathbf{g}_1(C_j) \mathbf{g}_1(C_j)'}{\sigma_2^2(\mathbf{P}_2\mathbf{P}'_2)_{jj}} + \mathbf{K}^{-1} \\
& \quad \text{and } \mathbf{b}' = \sum_{i=1}^{n_1} \frac{\mathbf{g}_1(B_i)' (Y_1(B_i) - \beta_1)}{\sigma_1^2(\mathbf{P}_1\mathbf{P}'_1)_{ii}} + \sum_{j=1}^{n_2} \frac{\beta_2 \mathbf{g}_1(C_j)' (Y_2(C_j) - \beta_0 - \beta_1\beta_2)}{\sigma_2^2(\mathbf{P}_2\mathbf{P}'_2)_{jj}} \\
& f(\beta_1 | \cdot) \propto \prod_{i=1}^{n_1} f(Y_1(B_i) | \beta_1, \boldsymbol{\eta}, \sigma_1^2) \cdot \prod_{j=1}^{n_2} f(Y_2(C_j) | \beta_0, \beta_1, \beta_2, \boldsymbol{\eta}, \sigma_2^2) \cdot f(\beta_1) \\
& \propto \exp \left(\sum_{i=1}^{n_1} -\frac{1}{2\sigma_1^2(\mathbf{P}_1\mathbf{P}'_1)_{ii}} (Y_1(B_i) - \beta_1 - \mathbf{g}_1(B_i)' \boldsymbol{\eta})^2 \right. \\
& \quad \left. - \sum_{j=1}^{n_2} \frac{1}{2\sigma_2^2(\mathbf{P}_2\mathbf{P}'_2)_{jj}} (Y_2(C_j) - \beta_0 - \beta_1\beta_2 - \beta_2\mathbf{g}_1(C_j)' \boldsymbol{\eta})^2 - \frac{1}{2\sigma_\beta^2} \beta_1^2 \right) \\
& \propto \exp \left[\beta_1^2 \left(-\sum_{i=1}^{n_1} \frac{1}{2\sigma_1^2(\mathbf{P}_1\mathbf{P}'_1)_{ii}} - \sum_{j=1}^{n_2} \frac{\beta_2^2}{2\sigma_2^2(\mathbf{P}_2\mathbf{P}'_2)_{jj}} - \frac{1}{2\sigma_\beta^2} \right) \right. \\
& \quad \left. - \beta_1 \left(-\sum_{i=1}^{n_1} \frac{Y_1(B_i) - \mathbf{g}_1(B_i)' \boldsymbol{\eta}}{\sigma_1^2(\mathbf{P}_1\mathbf{P}'_1)_{ii}} - \sum_{j=1}^{n_2} \frac{\beta_2 (Y_2(C_j) - \beta_0 - \beta_2 \mathbf{g}_1(C_j)' \boldsymbol{\eta})}{\sigma_2^2(\mathbf{P}_2\mathbf{P}'_2)_{jj}} \right) \right] \\
& = \exp(a\beta_1^2 - b\beta_1)
\end{aligned}$$

$$\begin{aligned}
&= \exp\left(\frac{\beta_1^2 - \frac{b}{a}\beta_1}{1/a}\right) \\
&= \exp\left(\frac{\beta_1^2 - 2\frac{b}{2a}\beta_1 + (\frac{b}{2a})^2 - (\frac{b}{2a})^2}{1/a}\right) \\
&\propto \exp\left(\frac{(\beta_1 - \frac{b}{2a})^2}{1/a}\right) \\
&= \exp\left(\frac{(\beta_1 - \frac{b}{2a})^2}{-2(-\frac{1}{2a})}\right) \\
&\propto N\left(\frac{b}{2a}, -\frac{1}{2a}\right) \quad \text{where } a = -\sum_{i=1}^{n_1} \frac{1}{2\sigma_1^2(\mathbf{P}_1\mathbf{P}'_1)_{ii}} - \sum_{j=1}^{n_2} \frac{\beta_2^2}{2\sigma_2^2(\mathbf{P}_2\mathbf{P}'_2)_{jj}} - \frac{1}{2\sigma_\beta^2} \\
&\quad \text{and } b = -\sum_{i=1}^{n_1} \frac{Y_1(B_i) - \mathbf{g}_1(B_i)'\boldsymbol{\eta}}{\sigma_1^2(\mathbf{P}_1\mathbf{P}'_1)_{ii}} - \sum_{j=1}^{n_2} \frac{\beta_2(Y_2(C_j) - \beta_0 - \beta_2\mathbf{g}_1(C_j)'\boldsymbol{\eta})}{\sigma_2^2(\mathbf{P}_2\mathbf{P}'_2)_{jj}}
\end{aligned}$$

$$\begin{aligned}
f(\beta_2|\cdot) &\propto \prod_{j=1}^{n_2} f(Y_2(C_j)|\beta_0, \beta_1, \beta_2, \boldsymbol{\eta}, \sigma_2^2) \cdot f(\beta_2) \\
&\propto \exp\left(\sum_{j=1}^{n_2} -\frac{1}{2\sigma_2^2(\mathbf{P}_2\mathbf{P}'_2)_{jj}}(Y_2(C_j) - \beta_0 - \beta_1\beta_2 - \beta_2\mathbf{g}_1(C_j)'\boldsymbol{\eta})^2 - \frac{1}{2\sigma_\beta^2}\beta_2^2\right) \\
&\propto \exp\left[\beta_2^2\left(\sum_{j=1}^{n_2} -\frac{(\beta_1 + \mathbf{g}_1(C_j)'\boldsymbol{\eta})^2}{2\sigma_2^2(\mathbf{P}_2\mathbf{P}'_2)_{jj}} - \frac{1}{2\sigma_\beta^2}\right) - \beta_2\left(-\sum_{j=1}^{n_2} \frac{(\beta_1 + \mathbf{g}_1(C_j)'\boldsymbol{\eta})(Y_2(C_j) - \beta_0)}{\sigma_2^2(\mathbf{P}_2\mathbf{P}'_2)_{jj}}\right)\right] \\
&= \exp(a\beta_2^2 - b\beta_2) \\
&= \exp\left(\frac{\beta_2^2 - \frac{b}{a}\beta_2}{1/a}\right) \\
&= \exp\left(\frac{\beta_2^2 - 2\frac{b}{2a}\beta_2 + (\frac{b}{2a})^2 - (\frac{b}{2a})^2}{1/a}\right) \\
&\propto \exp\left(\frac{(\beta_2 - \frac{b}{2a})^2}{1/a}\right) \\
&= \exp\left(\frac{(\beta_2 - \frac{b}{2a})^2}{-2(-\frac{1}{2a})}\right) \\
&\propto N\left(\frac{b}{2a}, -\frac{1}{2a}\right) \quad \text{where } a = \sum_{j=1}^{n_2} -\frac{(\beta_1 + \mathbf{g}_1(C_j)'\boldsymbol{\eta})^2}{2\sigma_2^2(\mathbf{P}_2\mathbf{P}'_2)_{jj}} - \frac{1}{2\sigma_\beta^2} \\
&\quad \text{and } b = -\sum_{j=1}^{n_2} \frac{(\beta_1 + \mathbf{g}_1(C_j)'\boldsymbol{\eta})(Y_2(C_j) - \beta_0)}{\sigma_2^2(\mathbf{P}_2\mathbf{P}'_2)_{jj}}
\end{aligned}$$

$$\begin{aligned}
f(\beta_0|\cdot) &\propto \prod_{j=1}^{n_2} f(Y_2(C_j)|\beta_0, \beta_1, \beta_2, \boldsymbol{\eta}, \sigma_2^2) \cdot f(\beta_0) \\
&\propto \exp\left(\sum_{j=1}^{n_2} -\frac{1}{2\sigma_2^2(\mathbf{P}_2\mathbf{P}'_2)_{jj}}(Y_2(C_j) - \beta_0 - \beta_1\beta_2 - \beta_2\mathbf{g}_1(C_j)'\boldsymbol{\eta})^2 - \frac{1}{2\sigma_\beta^2}\beta_0^2\right) \\
&\propto \exp\left[\beta_0^2\left(\sum_{j=1}^{n_2} -\frac{1}{2\sigma_2^2(\mathbf{P}_2\mathbf{P}'_2)_{jj}} - \frac{1}{2\sigma_\beta^2}\right) - \beta_0\left(-\sum_{j=1}^{n_2} \frac{Y_2(C_j) - \beta_1\beta_2 - \beta_2\mathbf{g}_1(C_j)'\boldsymbol{\eta}}{\sigma_2^2(\mathbf{P}_2\mathbf{P}'_2)_{jj}}\right)\right] \\
&= \exp(a\beta_0^2 - b\beta_0) \\
&= \exp\left(\frac{\beta_0^2 - \frac{b}{a}\beta_0}{1/a}\right) \\
&= \exp\left(\frac{\beta_0^2 - 2\frac{b}{2a}\beta_0 + (\frac{b}{2a})^2 - (\frac{b}{2a})^2}{1/a}\right) \\
&\propto \exp\left(\frac{(\beta_0 - \frac{b}{2a})^2}{1/a}\right) \\
&= \exp\left(\frac{(\beta_0 - \frac{b}{2a})^2}{-2(-\frac{1}{2a})}\right) \\
&\propto N\left(\frac{b}{2a}, -\frac{1}{2a}\right) \quad \text{where } a = \sum_{j=1}^{n_2} -\frac{1}{2\sigma_2^2(\mathbf{P}_2\mathbf{P}'_2)_{jj}} - \frac{1}{2\sigma_\beta^2} \\
&\quad \text{and } b = -\sum_{j=1}^{n_2} \frac{Y_2(C_j) - \beta_1\beta_2 - \beta_2\mathbf{g}_1(C_j)'\boldsymbol{\eta}}{\sigma_2^2(\mathbf{P}_2\mathbf{P}'_2)_{jj}}
\end{aligned}$$

$$\begin{aligned}
f(\sigma_\eta^2|\cdot) &\propto f(\boldsymbol{\eta}|\sigma_\eta^2, \phi) \cdot f(\sigma_\eta^2) \\
&\propto (\sigma_\eta^2)^{-a_\eta-1} \exp\left(-\frac{b_\eta}{\sigma_\eta^2}\right) \cdot |\{\sigma_\eta^2 \exp(-\phi\|\mathbf{c}_i - \mathbf{c}_j\|)\}|^{-1/2} \exp\left(-\frac{1}{2}\boldsymbol{\eta}'\{\sigma_\eta^2 \exp(-\phi\|\mathbf{c}_i - \mathbf{c}_j\|)\}^{-1}\boldsymbol{\eta}\right) \\
&\propto (\sigma_\eta^2)^{-a_\eta-1} \exp\left(-\frac{b_\eta}{\sigma_\eta^2}\right) (\sigma_\eta^2)^{-r/2} \exp\left(-\frac{1}{2\sigma_\eta^2}\boldsymbol{\eta}'\{\exp(-\phi\|\mathbf{c}_i - \mathbf{c}_j\|)\}^{-1}\boldsymbol{\eta}\right) \\
&= (\sigma_\eta^2)^{-(a_\eta + \frac{r}{2})-1} \exp\left(-\frac{b_\eta + \frac{1}{2}\boldsymbol{\eta}'\{\exp(-\phi\|\mathbf{c}_i - \mathbf{c}_j\|)\}^{-1}\boldsymbol{\eta}}{\sigma_\eta^2}\right) \\
&\propto IG\left(a_\eta + \frac{r}{2}, b_\eta + \frac{1}{2}\boldsymbol{\eta}'\{\exp(-\phi\|\mathbf{c}_i - \mathbf{c}_j\|)\}^{-1}\boldsymbol{\eta}\right)
\end{aligned}$$

$$\begin{aligned}
f(\sigma_1^2|\cdot) &\propto \prod_{i=1}^{n_1} f(Y_1(B_i)|\beta_1, \boldsymbol{\eta}, \sigma_1^2) \cdot f(\sigma_1^2) \\
&\propto \prod_{i=1}^{n_1} \left(\frac{1}{\sqrt{2\pi\sigma_1^2(\mathbf{P}_1\mathbf{P}'_1)_{ii}}} \exp\left(-\frac{(Y_1(B_i) - \beta_1 - \mathbf{g}_1(B_i)'\boldsymbol{\eta})^2}{2\sigma_1^2(\mathbf{P}_1\mathbf{P}'_1)_{ii}}\right)\right) \cdot (\sigma_1^2)^{-a_\sigma-1} \exp\left(-\frac{b_\sigma}{\sigma_1^2}\right) \\
&\propto (\sigma_1^2)^{-(a_\sigma + \frac{n_1}{2})-1} \exp\left(-\frac{b_\sigma + \sum_{i=1}^{n_1} \frac{1}{2(\mathbf{P}_1\mathbf{P}'_1)_{ii}}(Y_1(B_i) - \beta_1 - \mathbf{g}_1(B_i)'\boldsymbol{\eta})^2}{\sigma_1^2}\right)
\end{aligned}$$

$$\begin{aligned}
& \propto IG \left(a_\sigma + \frac{n_1}{2}, b_\sigma + \sum_{i=1}^{n_1} \frac{1}{2(\mathbf{P}_1 \mathbf{P}'_1)_{ii}} (Y_1(B_i) - \beta_1 - \mathbf{g}_1(B_i)' \boldsymbol{\eta})^2 \right) \\
f(\sigma_2^2 | \cdot) & \propto \prod_{j=1}^{n_2} f(Y_2(C_j) | \beta_0, \beta_1, \beta_2, \boldsymbol{\eta}, \sigma_2^2) \cdot f(\sigma_2^2) \\
& \propto \prod_{j=1}^{n_2} \left(\frac{1}{\sqrt{2\pi\sigma_2^2(\mathbf{P}_2 \mathbf{P}'_2)_{jj}}} \exp \left(-\frac{(Y_2(C_j) - \beta_0 - \beta_1\beta_2 - \beta_2 \mathbf{g}_1(C_j)' \boldsymbol{\eta})^2}{2\sigma_2^2(\mathbf{P}_2 \mathbf{P}'_2)_{jj}} \right) \right) \cdot (\sigma_2^2)^{-a_\sigma - 1} \exp \left(-\frac{b_\sigma}{\sigma_2^2} \right) \\
& \propto (\sigma_2^2)^{-(a_\sigma + \frac{n_2}{2}) - 1} \exp \left(-\frac{b_\sigma + \sum_{j=1}^{n_2} \frac{1}{2(\mathbf{P}_2 \mathbf{P}'_2)_{jj}} (Y_2(C_j) - \beta_0 - \beta_1\beta_2 - \beta_2 \mathbf{g}_1(C_j)' \boldsymbol{\eta})^2}{\sigma_2^2} \right) \\
& \propto IG \left(a_\sigma + \frac{n_2}{2}, b_\sigma + \sum_{j=1}^{n_2} \frac{1}{2(\mathbf{P}_2 \mathbf{P}'_2)_{jj}} (Y_2(C_j) - \beta_0 - \beta_1\beta_2 - \beta_2 \mathbf{g}_1(C_j)' \boldsymbol{\eta})^2 \right) \\
f(\phi | \cdot) & \propto f(\boldsymbol{\eta} | \sigma_\eta^2, \phi) \cdot f(\phi) \\
& \propto \{ \sigma_\eta^2 \exp(-\phi \|\mathbf{c}_i - \mathbf{c}_j\|) \}^{-1/2} \exp \left(-\frac{1}{2} \boldsymbol{\eta}' \{ \sigma_\eta^2 \exp(-\phi \|\mathbf{c}_i - \mathbf{c}_j\|) \}^{-1} \boldsymbol{\eta} \right) \cdot \frac{1}{b_\phi - a_\phi}
\end{aligned}$$

Again, ϕ does not have a closed form full conditional distribution, and thus requires a Metropolis-Hasting step to update.